AD NUMBER

ADB009356

LIMITATION CHANGES

TO:

Approved for public release; distribution is unlimited.

FROM:

Distribution authorized to U.S. Gov't. agencies only; Test and Evaluation; FEB 1976. Other requests shall be referred to Air Force Flight Dynamics Laboratory, Attn: AFFDL/FER, Wright-Patterson, AFB OH 45433.

AUTHORITY

AFWAL ltr, 6 Nov 1980

AEDC-TR-76-21

COMPARISON OF PARACHUTE PERFORMANCE AT TRANSONIC MACH NUMBERS FOR CONICAL RIBBON PARACHUTES CONSTRUCTED OF NYLON AND KEVLAR-29 MATERIALS

PROPULSION WIND TUNNEL FACILITY
ARNOLD ENGINEERING DEVELOPMENT CENTER
AIR FORCE SYSTEMS COMMAND
ARNOLD AIR FORCE STATION, TENNESSEE

February 1976

Final Report for Period 16 – 19 September, 1975

Prepared for

AIR FORCE FLIGHT DYNAMICS LABORATORY (FER)
WRIGHT-PATTERSON AIR FORCE BASE, OHIO 45433

NOTICES

When U. S. Government drawings specifications, or other data are used for any purpose other than a definitely related Government procurement operation, the Government thereby incurs no responsibility nor any obligation whatsoever, and the fact that the Government may have formulated, furnished, or in any way supplied the said drawings, specifications, or other data, is not to be regarded by implication or otherwise, or in any manner licensing the holder or any other person or corporation, or conveying any rights or permission to manufacture, use, or sell any patented invention that may in any way be related thereto.

Qualified users may obtain copies of this report from the Defense Documentation Center.

References to named commercial products in this report are not to be considered in any sense as an endorsement of the product by the United States Air Force or the Government.

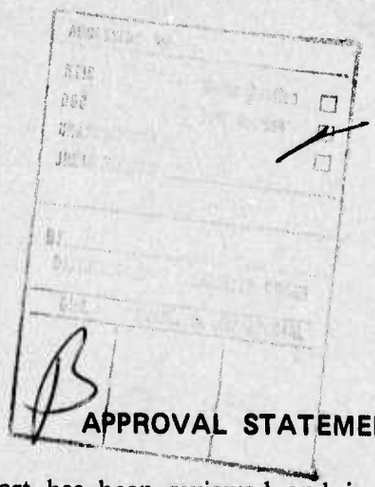

APPROVAL STATEMENT

This technical report has been reviewed and is approved for publication.

FOR THE COMMANDER

John C. Cardosi

JOHN C. CARDOSI
Lt Colonel, USAF
Chief Air Force Test Director, PWT
Directorate of Test

Craig E. Mahaffy

CRAIG E. MAHAFFY
Colonel, USAF
Director of Test

UNCLASSIFIED

REPORT DOCUMENTATION PAGE	READ INSTRUCTIONS BEFORE COMPLETING FORM
1 REPORT NUMBER: AEDC-TR-76-21	2 GOVT ACCESSION NO. / 3 RECIPIENT'S CATALOG NUMBER
4 TITLE (and Subtitle): COMPARISON OF PARACHUTE PERFORMANCE AT TRANSONIC MACH NUMBERS FOR CONICAL RIBBON PARACHUTES CONSTRUCTED OF NYLON AND KEVLAR-29 MATERIALS	5 TYPE OF REPORT & PERIOD COVERED: Final Report, 16 - 19 September 1975
	6 PERFORMING ORG. REPORT NUMBER
7 AUTHOR(S): W. L. Peters, ARO, Inc.	8 CONTRACT OR GRANT NUMBER(S)
9 PERFORMING ORGANIZATION NAME AND ADDRESS: Arnold Engineering Development Center (XO) Air Force Systems Command Arnold Air Force Station, TN 37389	10 PROGRAM ELEMENT, PROJECT, TASK AREA & WORK UNIT NUMBERS: Program Element 62201F Project 6065 Task 03
11 CONTROLLING OFFICE NAME AND ADDRESS: Air Force Flight Dynamics Laboratory (AFFDL/FER), Wright-Patterson Air Force Base, OH 45433	12 REPORT DATE: February 1976 / 13 NUMBER OF PAGES: 42
14 MONITORING AGENCY NAME & ADDRESS (if different from Controlling Office)	15 SECURITY CLASS. (of this report): UNCLASSIFIED
	15a DECLASSIFICATION DOWNGRADING SCHEDULE: N/A

16 DISTRIBUTION STATEMENT (of this Report)
Distribution limited to U.S. Government agencies only; this report contains information on test and evaluation of military hardware; February 1976; other requests for this document must be referred to Air Force Flight Dynamics Laboratory (AFFDL/FER), Wright-Patterson AFB, OH 45433.

17 DISTRIBUTION STATEMENT (of the abstract entered in Block 20, if different from Report)

18 SUPPLEMENTARY NOTES
Available in DDC.

19 KEY WORDS (Continue on reverse side if necessary and identify by block number)
parachute fabrics
drag chutes
ribbon parachutes
transonic flow
drag

20 ABSTRACT (Continue on reverse side if necessary and identify by block number)
Tests were conducted in the ~~AEDC~~ Propulsion Wind Tunnel (~~4GT~~) to determine deployment and inflation characteristics which would allow comparative performance evaluations to be made of four conical ribbon parachute versions constructed of either nylon and/or Kevlar-29 materials. Dynamic deployment data were obtained at a nominal Mach number of 0.8 and dynamic pressures from 200 to 800 psf, and steady-state data were obtained at Mach numbers from 0.6

DD FORM 1 JAN 73 1473 EDITION OF 1 NOV 65 IS OBSOLETE

UNCLASSIFIED

042550

20. ABSTRACT (Continued)

to 1.2 and dynamic pressures from 200 to 650 psf. In general, parachutes constructed of Kevlar-29 material withstood the same opening shock loads while exhibiting a shorter damping time for inflation drag loads compared with nylon-constructed chutes. The least postinflation drag dynamics were exhibited by those parachutes which contained Kevlar-29 materials. A significant savings in weight and volume was realized by using Kevlar-29 as a substitute for nylon in parachute construction.

AFSC
Arnold AFS Tenn

PREFACE

The work reported herein was conducted by the Arnold Engineering Development Center (AEDC), Air Force Systems Command (AFSC), at the request of the Air Force Flight Dynamics Laboratory (AFFDL/FER), under Program Element 62201F. The results of the test were obtained by ARO, Inc. (a subsidiary of Sverdrup & Parcel and Associates, Inc.), contract operator of AEDC, AFSC, Arnold Air Force Station, Tennessee, under ARO Project Number P41S-17A. The author of this report was W. L. Peters, ARO, Inc. The data reduction was completed on October 13, 1975, and the manuscript (ARO Control No. ARO-PWT-TR-75-160) was submitted for publication on November 11, 1975.

CONTENTS

ILLUSTRATIONS

Figure | Page

TABLES

1.0 INTRODUCTION

The objective of this test program was to acquire deployment, inflation, and steady-state data which would allow further comparative evaluations to be made of nylon and Kevlar-29 (formerly denoted Fiber B) conical ribbon parachute. A total of 28 deployments of nylon, nylon/Kevlar-29, and Kevlar-29 parachutes were made from a strut-mounted cylindrical forebody with a flared base section at Mach numbers from 0.6 to 1.2 and dynamic pressures from 200 to 800 psf.

2.0 APPARATUS

2.1 TEST FACILITY

The AEDC Propulsion Wind Tunnel (16T) is a closed-circuit, continuous flow wind tunnel capable of operation between Mach numbers 0.20 and 1.60. The tunnel can be operated over a stagnation pressure range from 120 to 4,300 psfa, depending on Mach number. The test section stagnation temperature can be controlled through a range of about 80 to 160°F by varying the cooling water temperature. The wind tunnel specific humidity is controlled by removing tunnel air and supplying makeup air from an atmospheric dryer. A more complete description of the wind tunnel and its operating characteristics can be found in Ref. 1.

A sketch showing the model location and strut support arrangement in Tunnel 16T is presented in Fig. 1.

2.2 TEST ARTICLES

2.2.1 Model Forebody and Deployment System

The parachutes were deployed from a strut-mounted forebody as shown in a dimensioned sketch and a test section installation photograph in Figs. 2 and 3, respectively. An ogive nose section is normally used on the forebody; however, for this test program as well as for the similar previous test program reported in Ref. 2, the nose was removed so that air flowing through the forebody could assist the deployment spring system. A further modification was made to the forebody for the present test program with the incorporation of a forebody inlet and an internal butterfly valve to control airflow through the forebody. The butterfly valve was operative in only a completely open or closed mode through actuation of an air cylinder. Air pressure to the cylinder was controlled by means of two solenoid valves. A sketch of the forebody inlet and butterfly valve is shown in Fig. 4.

The parachute package was placed in the forebody storage compartment located in the flared base section of the model and was restrained against a spring-loaded plate by four straps. These straps were connected by a release pin mechanism to deploy the parachute package at activation of the same air cylinder utilized by the butterfly valve. The riser webs of the parachutes were fastened by two pins to a load cell arrangement located in the model forebody. A sketch of the load cell arrangement is shown in Fig. 5.

2.2.2 Parachute Details

The parachute design utilized for this test program was like that for the previous test program reported in Refs. 2 and 3. This design is representative of the strength and size range commonly used for drogue parachutes. Each parachute tested was of the conical ribbon type with a nominal diameter of 6.4 ft, a 20-deg cone angle, and a geometric porosity of 15 percent. The general characteristics of the parachute design are presented in Fig. 6.

Sixteen parachutes of four different versions were tested with each version differing in the percentages by weight in the amount of nylon and/or Kevlar-29 materials used in construction. The material makeup of each of the components of the four parachute construction versions is listed in Table 1. With the exception of the riser webs, similar components among the four versions were constructed of equal tensile strength whether composed of nylon or Kevlar-29 materials. The Kevlar-29 riser webs were constructed of one-half the strength of their nylon counterparts.

Some of the physical properties of Kevlar-29 are listed in Table 2 along with similar properties for the common parachute materials of nylon and Dacron®. As shown, a filament of Kevlar-29 has approximately 3.5 times larger ultimate tensile strength than a nylon or a Dacron filament. This indicates that a weight savings is realized in the construction of parachutes if Kevlar-29 is used as an equal strength replacement for either of these materials. Also, Kevlar-29 gives an even greater volume savings since its specific gravity is higher than that of nylon or Dacron. The weight and storage volume reduction achieved by using Kevlar-29 wholly or partially for the four different construction parachute versions in this test program is shown in Fig. 7. As shown, a maximum saving of 60 percent in weight and 68 percent in volume is realized by using all Kevlar-29 parachute components compared to using all nylon parachute components.

2.3 INSTRUMENTATION

The parachute drag load was measured by a 20,000-lb capacity, dual element load cell. The outputs from the load cell were digitized and recorded on magnetic tape for

online, steady-state data reduction and were recorded by a high-speed digital data recording system at a sampling rate of approximately 2,500 samples per second for offline data reduction of parachute drag dynamics. These outputs were also continuously recorded on direct-writing oscillographs for real time monitoring of load dynamics.

Five motion-picture cameras and a 70-mm still camera visually documented the test, and television cameras were utilized to monitor the forebody and parachutes during the test.

3.0 PROCEDURE

3.1 TEST CONDITIONS AND TECHNIQUE

Before the initiation of the wind tunnel test operation, the parachute package was installed in the forebody storage compartment and the air cylinder was actuated to close the butterfly valve within the forebody. After test conditions were achieved, a countdown procedure was used to sequence data acquisition during deployment of the parachute. The deployment procedure consisted of activation of the oscillographs, the high-speed digital recording system, and the motion-picture cameras, followed by the actuation of the air cylinder to open the butterfly valve and initiate the release pin mechanism to deploy the parachute. After inflation of the chute, steady-state drag loads were acquired by electrically averaging the load cell analog output over an interval of 1 sec.

The steady-state drag data were reduced to coefficient form by using a reference area based on the nominal parachute diameter of 6.4 ft and the tunnel test dynamic pressure values acquired after inflation of the parachute. In Fig. 8, the deterioration of Mach number and dynamic pressure with the sudden increase in tunnel blockage resulting from parachute inflation is shown. A maximum decrease of 26 percent in Mach number and 24 percent in dynamic pressure were experienced with parachute inflation at a predeployment Mach number of 1.2 and a dynamic pressure of 350 psf. The postdeployment (approximately 2 sec after deployment) dynamic drag performance parameters, such as standard deviation, average drag coefficient, skewness, and kurtosis were calculated from the data recorded by the high-speed recording system utilizing the statistical analysis program which is outlined in Ref. 4.

A summary of parachute deployments is presented in Table 3 with the nominal tunnel conditions prior to the time of deployment listed for all configurations tested. Drag data were obtained for designated configurations at Mach numbers from 0.6 to 1.2 at dynamic pressures ranging from 200 to 650 psf as shown in Table 4. The model forebody angle of attack and angle of sideslip were zero at all test conditions.

3.2 UNCERTAINTY OF MEASUREMENTS

Presented below is an estimate of the uncertainty of measurements based on nominal predeployment test conditions at a Mach number of 0.8 and a dynamic pressure of 350 psf. Values for drag uncertainty are given for both the online steady-state data and the data obtained on the high-speed recording system. The uncertainties of the parameters are presented for a 95-percent confidence level.

		Uncertainty (±)	
Parameter	Value	Online Steady-State Data	High-Speed Recording System Data
M_∞	0.8	0.003	0.003
q_∞, psf	350	2.2	2.2
D_o, lb	9000	13.71	37.61
C_{D_o}	0.8	0.00518	0.00633

4.0 RESULTS AND DISCUSSION

4.1 PARACHUTE DYNAMIC CHARACTERISTICS

Typical deployment drag time traces of the four parachute construction versions at a deployment Mach number of 0.8 and at dynamic pressures from 200 to 800 psf are presented in Fig. 9. The traces display the relative time for deployment as referenced to the time of air cylinder actuation and indicate the associated dynamics experienced by each parachute during deployment and inflation. The traces show that each parachute undergoes an initial deployment load, the snatch load, which occurs at the full extension of the riser webs and suspension lines, and that each chute encounters a maximum, or an opening shock load, which occurs at the full inflation of the canopy.

In Fig. 9, it is shown that parachutes constructed wholly or partially of Kevlar-29 display a shorter damping time for opening shock load dynamics than do chutes constructed of nylon. This characteristic is similar to that observed in the previous evaluation test of Kevlar-29 as a parachute material (Ref. 2). The shorter damping time is perhaps attributable to the greater stiffness of Kevlar-29, as presented in Table 2, with the material exhibiting approximately one-third less elongation under ultimate tensile loading as compared to nylon.

In Fig. 10, the opening shock loads for each of the Kevlar-29-constructed parachutes are compared to those for the all-nylon chutes as a function of predeployment dynamic

pressure. As shown, opening shock load linearly increases with dynamic pressure for the all-nylon parachute version. The chutes partially constructed of Kevlar-29 follow a similar trend but exhibit significantly smaller loads than the all-nylon chutes at dynamic pressures above 400 psf. These results show also that the all-Kevlar-29 parachutes display smaller opening shock loads than the all-nylon parachutes at dynamic pressures above 200 psf. The lower shock loads of the Kevlar-29 parachutes can again be attributed to the smaller elongation of Kevlar-29 material as compared to nylon. At lower dynamic pressures and loads, the difference in elongation is apparently not significant, but as dynamic pressure increases and opening shock loads become higher, the difference in elongation between nylon and Kevlar-29 becomes important. These higher loads result in a larger mouth diameter for the nylon chutes due to stretching of the components that make up the canopy and thus create a larger drag-producing surface for the nylon chutes.

With Kevlar-29 material exhibiting less than one-third of the elongation of nylon, an important concern of this test was whether Kevlar-29 parachutes could absorb opening shock load energy as well as nylon chutes. From Figs. 9 and 10, it is observed that the Kevlar-29 chutes withstood similar opening shock loads as well as the nylon chutes.

Several of the parachutes tested failed structurally during deployment and canopy inflation and are noted in Table 3. Most of the damage experienced by these chutes was in the form of failure in the horizontal ribbons, vertical tapes, and suspension lines.

The postinflation parachute drag dynamic characteristics (approximately 2 sec after deployment) of each parachute were determined from the statistical analysis program which reduces the drag data recorded by a high-speed digital data recording system at a sampling rate of 2,500 samples per second and calculates the drag distribution parameters of kurtosis, skewness, standard deviation, and the average drag coefficient. These parameters are tabulated on the dynamic drag coefficient distribution sample plot presented in Fig. 11 and are summarized in Table 5. Also presented is the 95-percent confidence level interval, which can be interpreted as representing a quantitative measurement of drag dynamics at a 95-percent confidence level. The drag dynamics of the test parachutes can be compared by each parachute's relative dynamic parameter (RDP), which is found by dividing the 95-percent confidence interval, expressed as the drag coefficient interval, by the average drag coefficient. These values are also tabulated in Table 5. The significance of the relative dynamic parameter can be shown by reviewing the drag dynamic characteristics of a parachute having a Gaussian-type drag distribution when values of zero, unity, and two are assigned to the relative dynamic parameter. A value of zero implies no dynamics; a value of unity implies that the magnitude of the dynamics about the average drag coefficient is equal to 50 percent of the average drag coefficient; a value of two implies that the magnitude of the dynamics about the average is equal to 100 percent of the average drag coefficient.

The deviation of the skewness parameter from zero indicates that the statistical distribution is not symmetrical about the average drag coefficient. Positive values of this parameter indicate higher dynamics above the average value, and likewise, negative values indicate lower dynamics than the average value. A value of three for the kurtosis parameter represents a typical Gaussian-type statistical distribution. If the kurtosis parameter is greater than three, the distribution is more peaked than a Gaussian distribution; likewise, if the kurtosis parameter has a value less than three, the distribution is less peaked than a Gaussian distribution.

The statistical analysis data in Table 5 and Fig. 12 show that as dynamic pressure increases from 200 to 600 psf, the four parachute versions display a decrease in the relative dynamic parameter and the standard deviation. It appears also that on the average the magnitudes of the relative dynamic parameter and the standard deviation become smaller as a function of increasing the amount of Kevlar-29 used in chute construction. These results thus indicate that a small reduction in postinflation drag dynamics can be achieved by using Kevlar-29 in place of nylon as a chute material.

4.2 STEADY-STATE PERFORMANCE

For this test program, free-stream flow was ducted through the deployment forebody so that dynamic pressure forces could assist in parachute deployment. In Fig. 13 the effect of this procedure on parachute drag is shown. These results were obtained by setting a given tunnel condition and by successively acquiring steady-state drag data with the butterfly valve open and closed. These data show that there is negligible change in steady-state drag performance with or without free-stream flow through the forebody at the various Mach numbers tested.

Presented in Fig. 14 is the variation of steady-state drag coefficient as a function of Mach number for the four parachute construction versions tested. In general, these data show that Kevlar-29-constructed parachutes exhibit less drag than nylon chutes at all Mach numbers and dynamic pressures. It appears also that this drag decrement between nylon and Kevlar-29 constructed chutes becomes larger as dynamic pressure increases. The lower drag of Kevlar-29 parachutes is a result of a smaller parachute mouth diameter, which in turn is attributable to the smaller elongation of Kevlar-29 as compared to nylon in the components that comprise the canopy.

The results in Fig. 14 show that except for Mach numbers between 0.7 and 0.9, the steady-state drag decreases slightly as Mach number increases for all parachute versions. At dynamic pressures of 200 and 350 psf, however, a marked decrease in drag from 0.7 to 0.8 Mach number is observed followed by a similar increase in drag from 0.8 to 0.9.

All parachute configurations in Fig. 14 for which steady-state drag results were obtained were tested until major parachute damage occurred. For most configurations this damage consisted of structural failure of the horizontal ribbons and vertical tapes within the canopy. These configurations are designated in Fig. 14 at the test conditions where damage was observed by online television cameras. Whenever parachute damage was noted, testing was terminated for the given parachute configuration. Since the results in Fig. 14 show no significant degradation in drag for these data, they are considered valid.

Though parachutes constructed of Kevlar-29 exhibit less drag than similarly constructed chutes of nylon, a significant weight and volume savings can be realized by using Kevlar-29 as a substitute for nylon, as shown in Figs. 15 and 16. Included are data from Ref. 2 for parachute construction versions NNBN, BNNN, and NBBN. These results show that a maximum weight savings of 57 percent and a volume savings of 65 percent can be achieved by using Kevlar-29 to construct a parachute with drag performance equivalent to that of an all-nylon chute. Because Kevlar-29 chutes exhibit lower drag than all-nylon chutes of equivalent size and strength, these savings are slightly less than predicted in Fig. 7 and are reduced further as dynamic pressure increases.

5.0 CONCLUDING REMARKS

Tests were conducted to evaluate the deployment and inflation characteristics, dynamics, and drag of parachutes constructed of Kevlar-29. The tests were conducted at Mach numbers from 0.6 to 1.2 and dynamic pressures from 200 to 800 psf. The following observations summarize the results:

1. A maximum savings of 57 percent in weight and 65 percent in volume can be realized by using Kevlar-29 as a substitute for nylon in parachute construction.

2. Opening shock loads for the all-nylon parachute version linearly increased with dynamic pressure. All of the Kevlar-29 parachute versions displayed significantly smaller opening shock loads than the all-nylon version above a dynamic pressure of 400 psf.

3. Kevlar-29-constructed parachutes absorbed opening shock loads as well as all-nylon-constructed parachutes.

4. Parachutes partially or wholly composed of Kevlar-29 generally exhibited less steady-state drag than the all-nylon-constructed parachutes at the same dynamic pressures. As dynamic pressure increased, this decrement in steady-state drag became larger.

5. The damping time for the deployment drag dynamics was shorter for Kevlar-29-constructed parachutes than for all-nylon-constructed parachutes.

6. A small reduction in postinflation drag dynamics was achieved by using Kevlar-29 in place of nylon as a chute material.

REFERENCES

1. Test Facilities Handbook (Tenth Edition). "Propulsion Wind Tunnel Facility, Vol. 4." Arnold Engineering Development Center, May 1974.

2. Peters W. L. "Effect of a High Strength-to-Weight Ratio Material on Parachute Performance at Mach Number 0.8." AEDC-TR-73-184 (AD914659L), November 1973.

3. Williams, Dale. "Investigation of Fiber B as a Lightweight Parachute Recovery System Material." GER-16012, April 1974.

4. Galigher, Lawrence L. "Aerodynamic Characteristics of Ballutes and Disk-Gap-Band Parachutes at Mach Numbers from 1.8 to 3.7." AEDC-TR-69-245 (AD861437), November 1969.

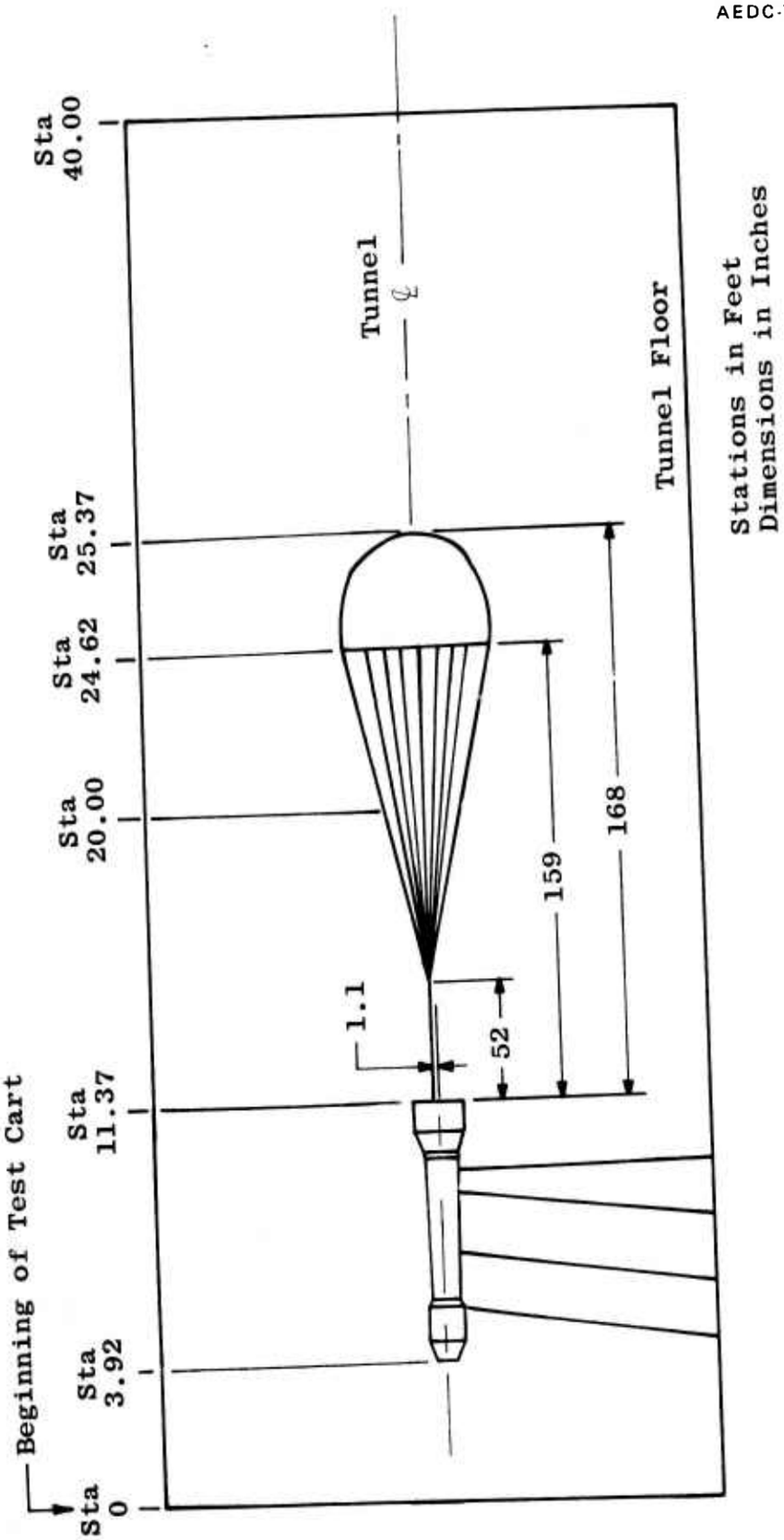

Figure 1. Model location in test section.

ERRATA

AEDC-TR-76-21, February 1976
(UNCLASSIFIED REPORT)

COMPARISON OF PARACHUTE PERFORMANCE AT TRANSONIC MACH NUMBERS FOR CONICAL RIBBON PARACHUTES CONSTRUCTED OF NYLON AND KEVLAR-29 MATERIALS

W. L. Peters, ARO, Inc.

Arnold Engineering Development Center
Air Force Systems Command
Arnold Air Force Station, Tennessee

B0093566

Please substitute the revised version of Figure 2 printed below for that on page 14 of subject report.

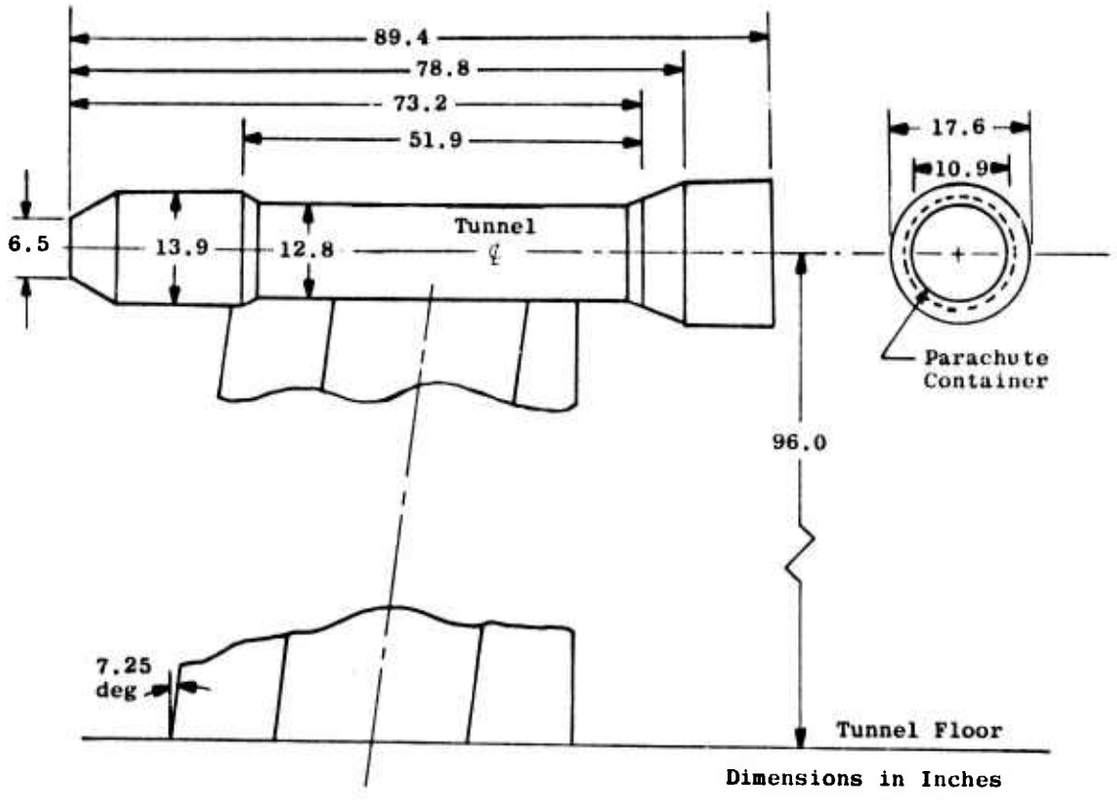

Figure 2. Sketch of model forebody.

14

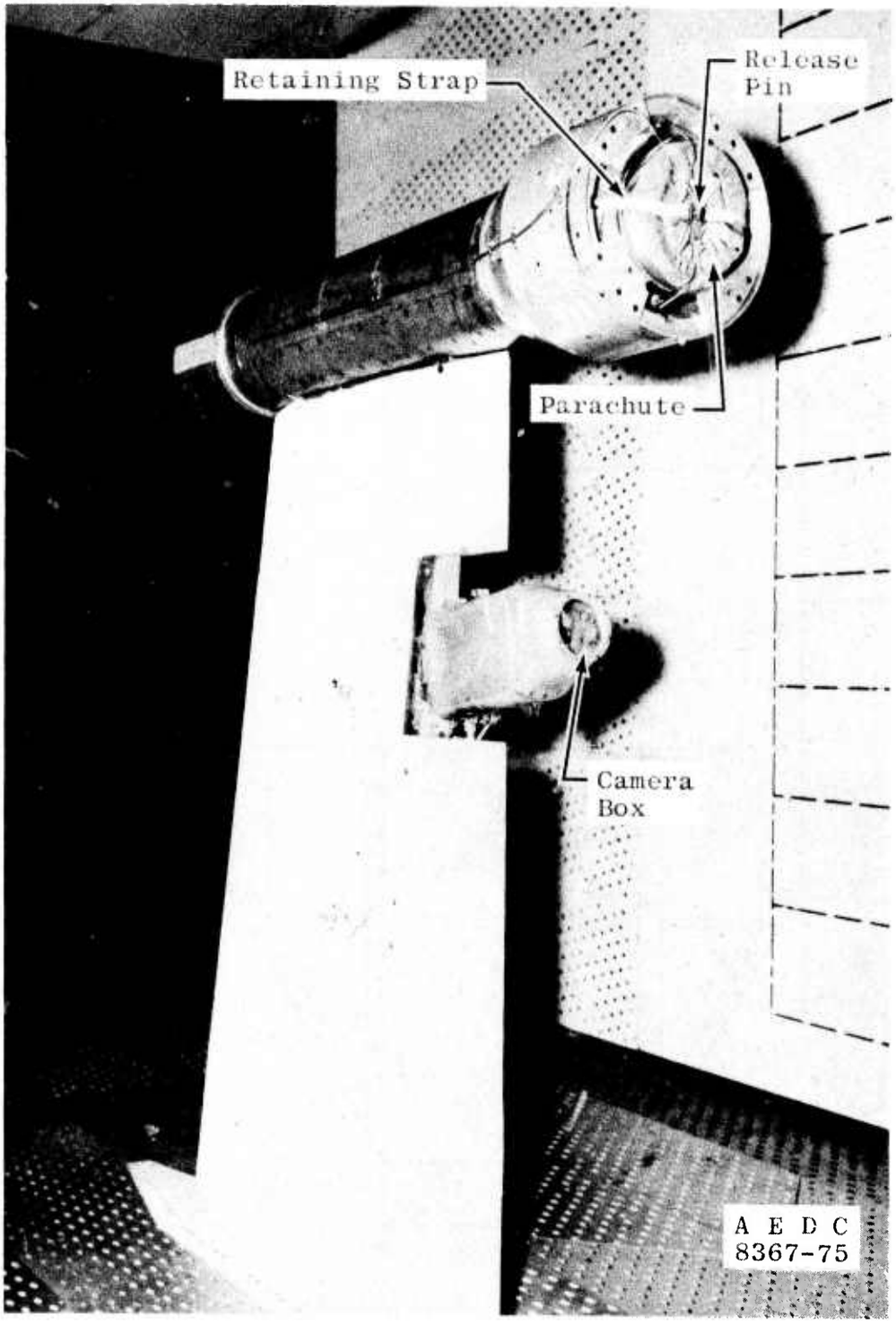

Figure 3. Installation of model forebody in test section.

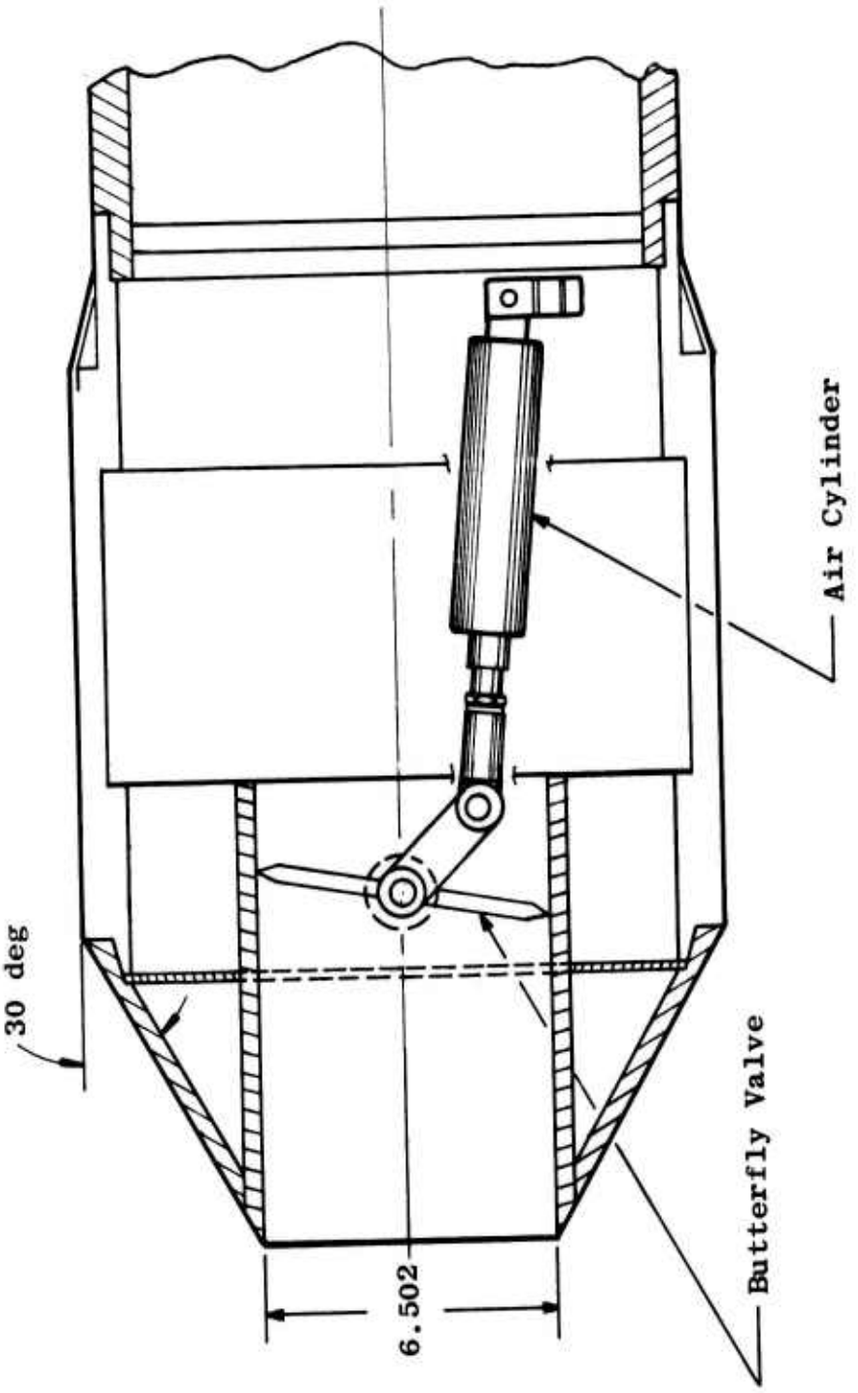

Figure 4. Sketch of forebody inlet and butterfly valve.

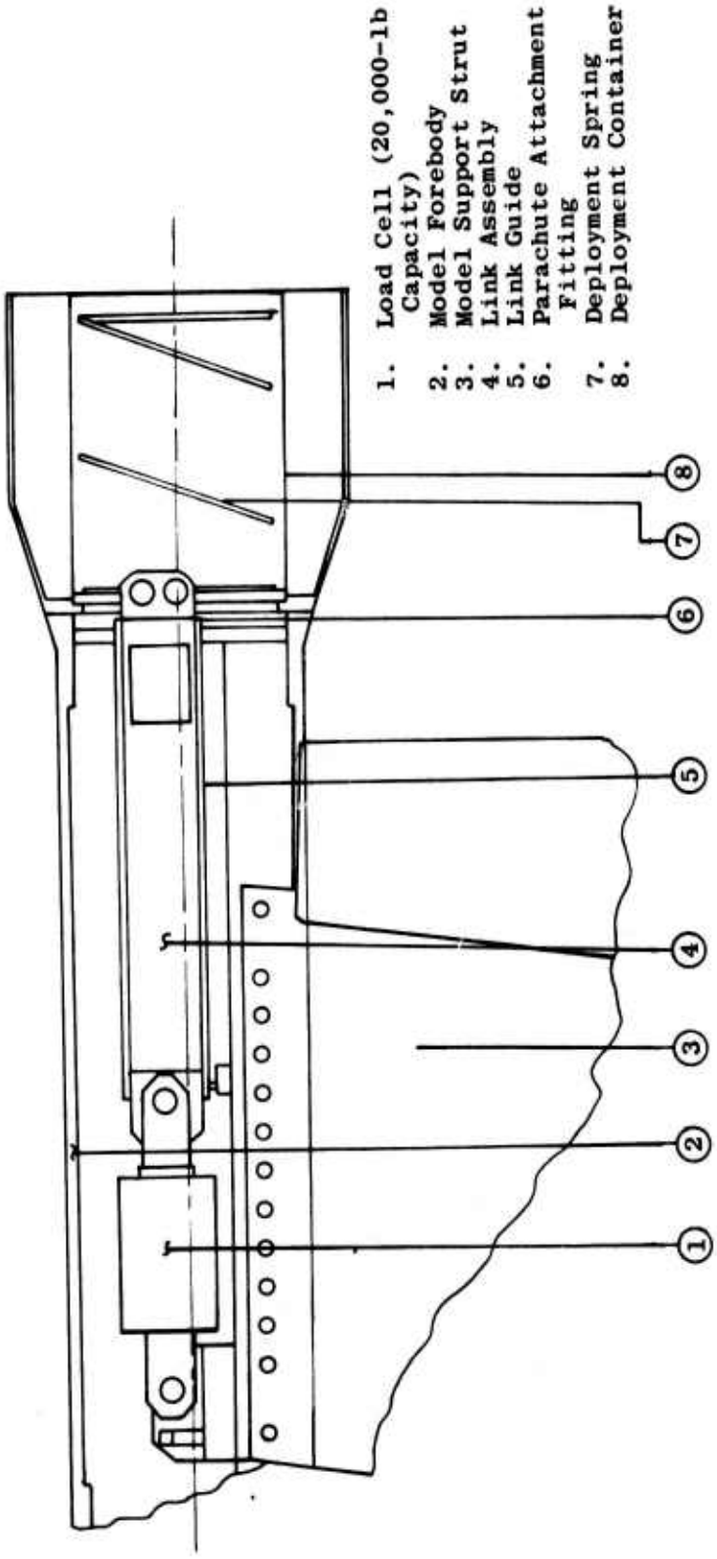

Figure 5. Sketch showing load cell installation.

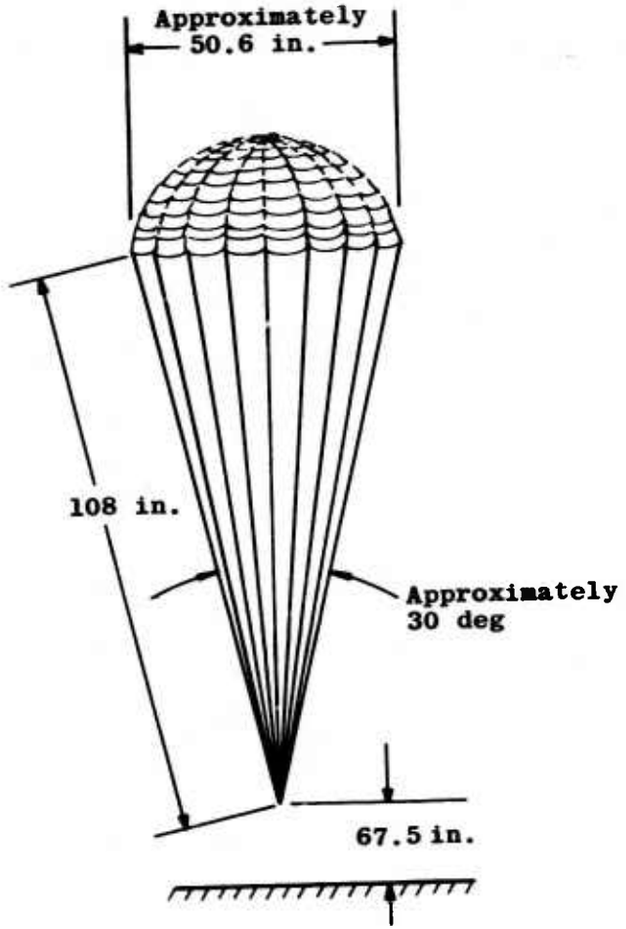

Characteristics

Type	20-deg Conical Ribbon
Nominal Diameter	6.4 ft
Geometric Porosity	15 percent
Number of Gores	16
Number of Lines	16
Line Length	108 in.
Line Strength (Individual)	1,500 lb
Riser Length	67.5 in.
Riser Strength	64,000 lb (Nylon) 32,000 lb (Kevlar-29)
Number of Horizontal Ribbons	14
Design Limit Load	9,600 lb
Proof Load	14,400 lb
Number of Verticals per Gore	3

Figure 6. Sketch of test parachute.

Note: Weight and volume of riser webs and keepers are excluded from these graphs.

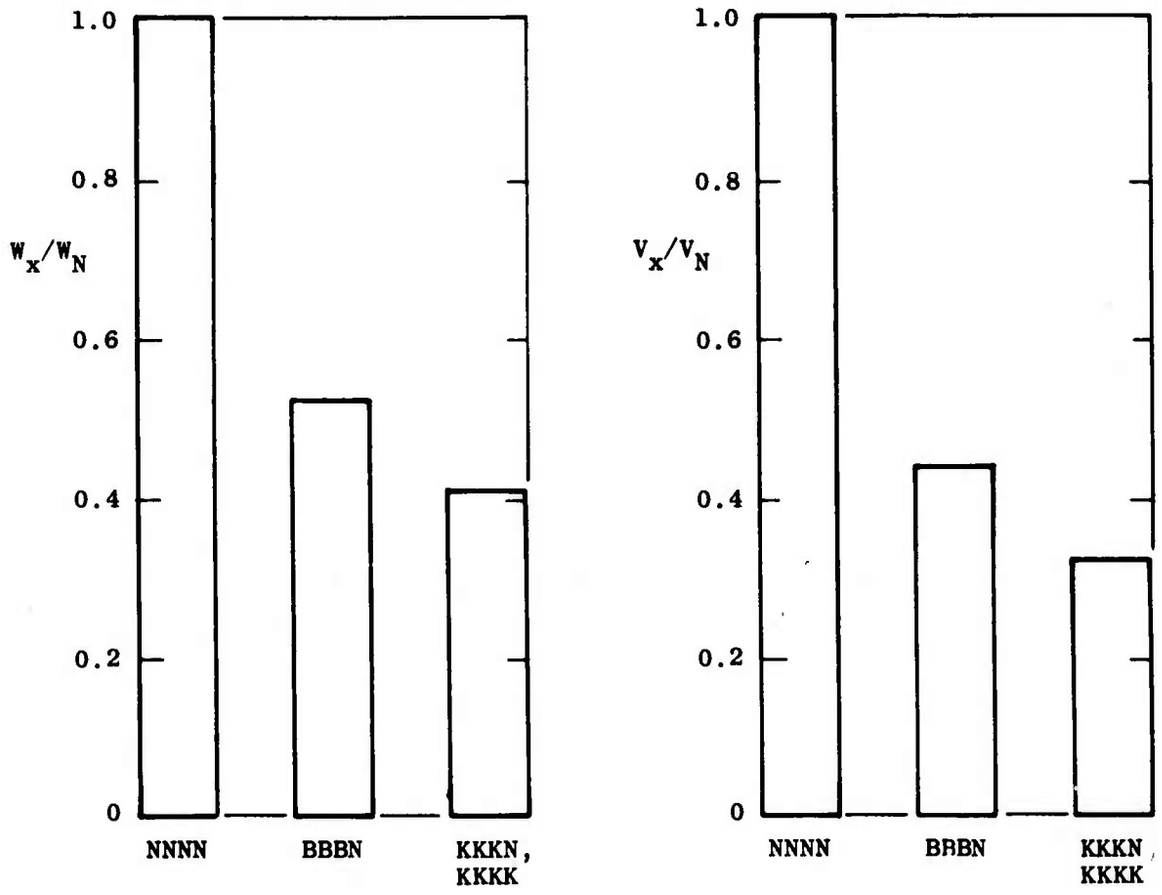

Figure 7. Weight and volume comparisons of the parachute construction versions tested.

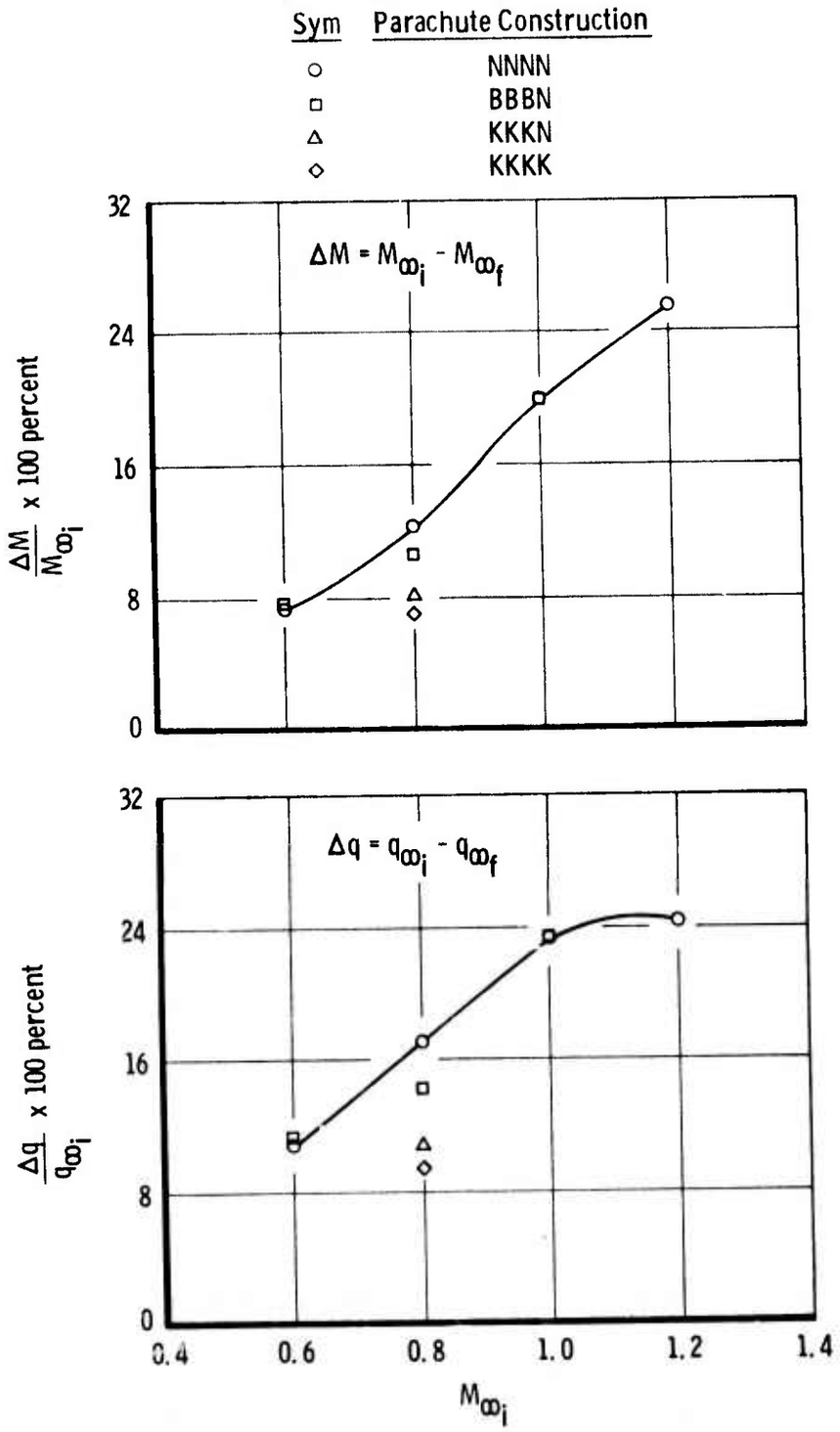

Figure 8. Effect of parachute inflation on free-stream tunnel conditions, $q_{\infty i}$ = 350 psf.

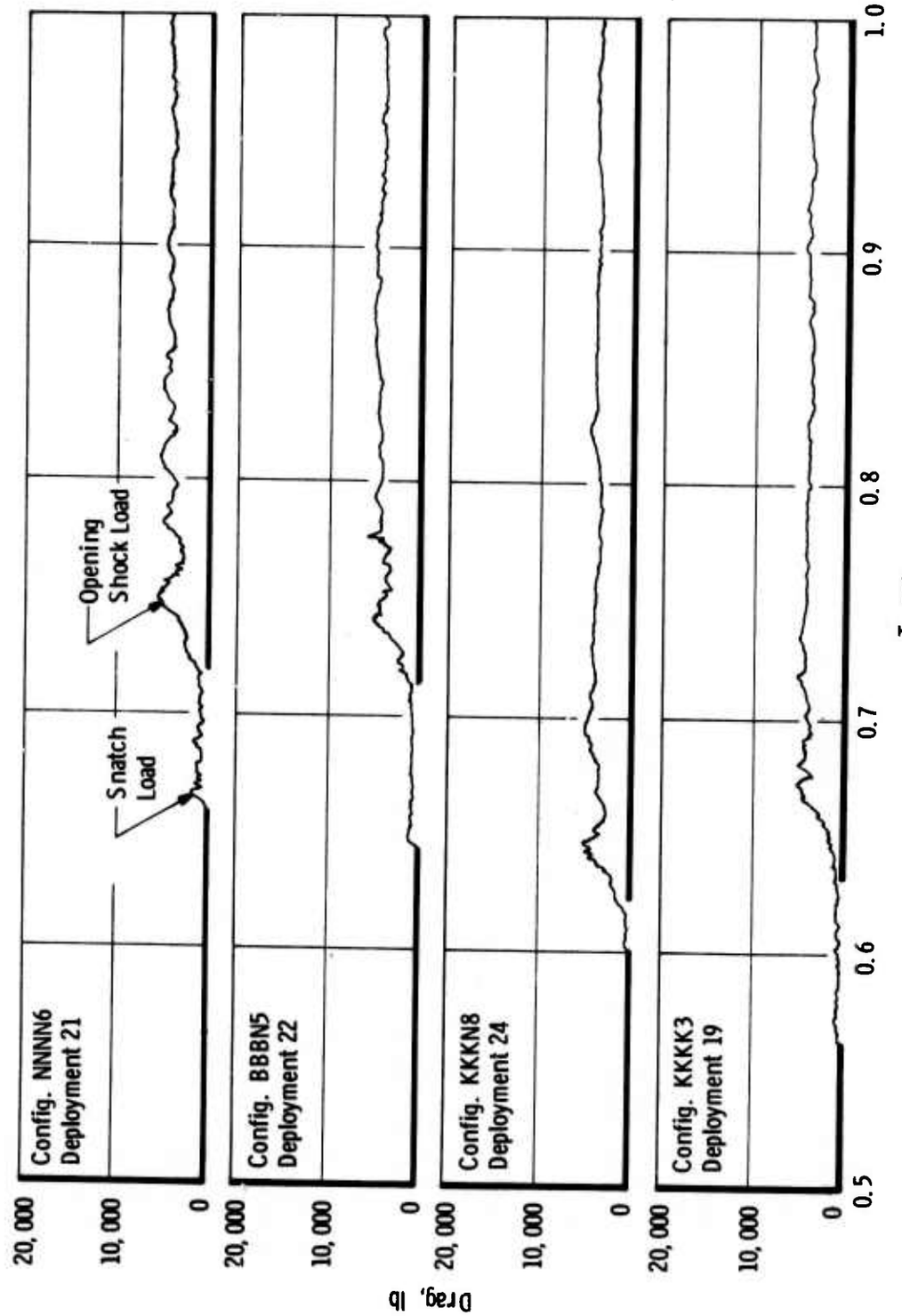

a. q_{∞_j} = 200 psf

Figure 9. Deployment characteristics of various parachute configurations, M_{∞_j} = 0.8.

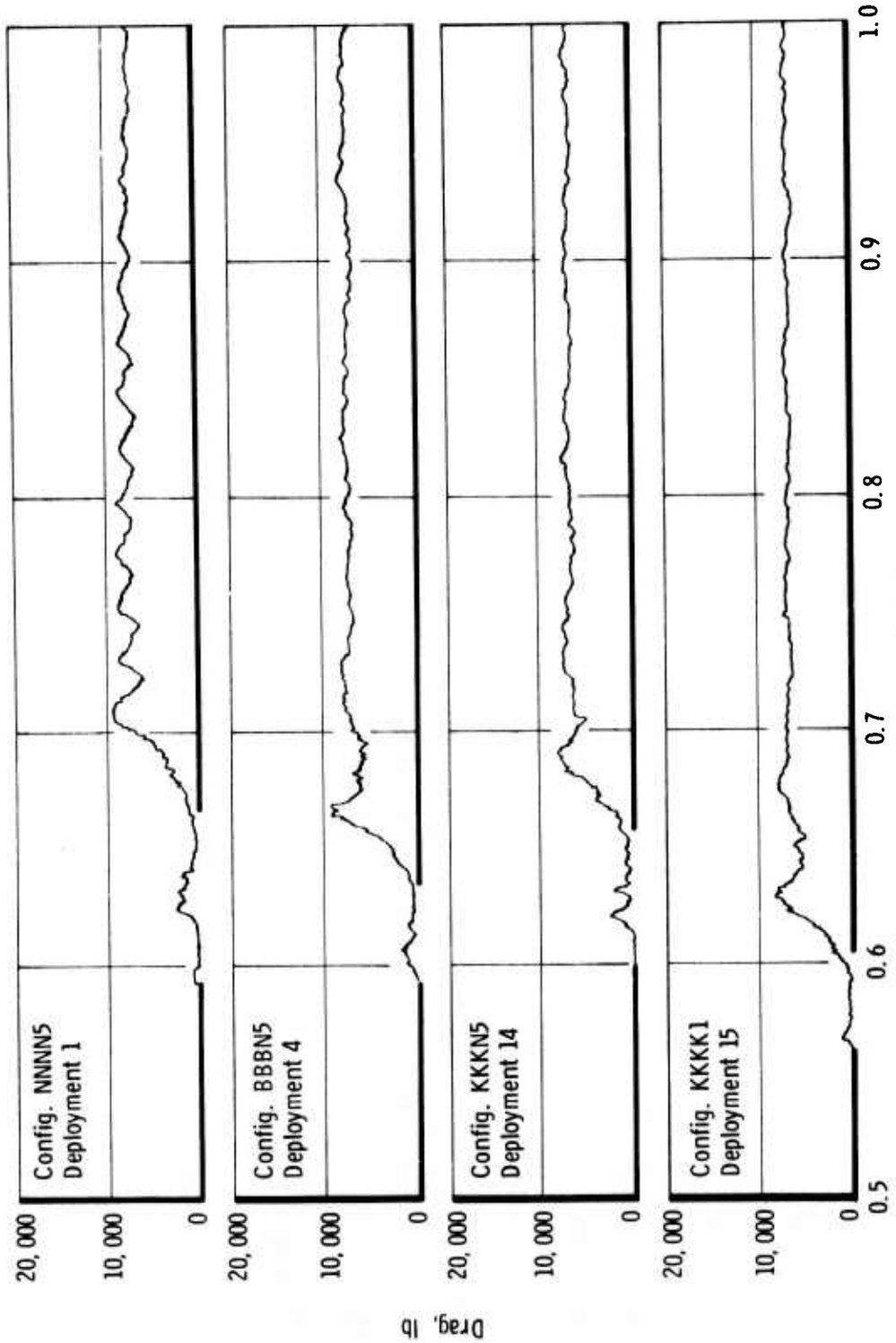

b. q_{∞_i} = 350 psf
Figure 9. Continued.

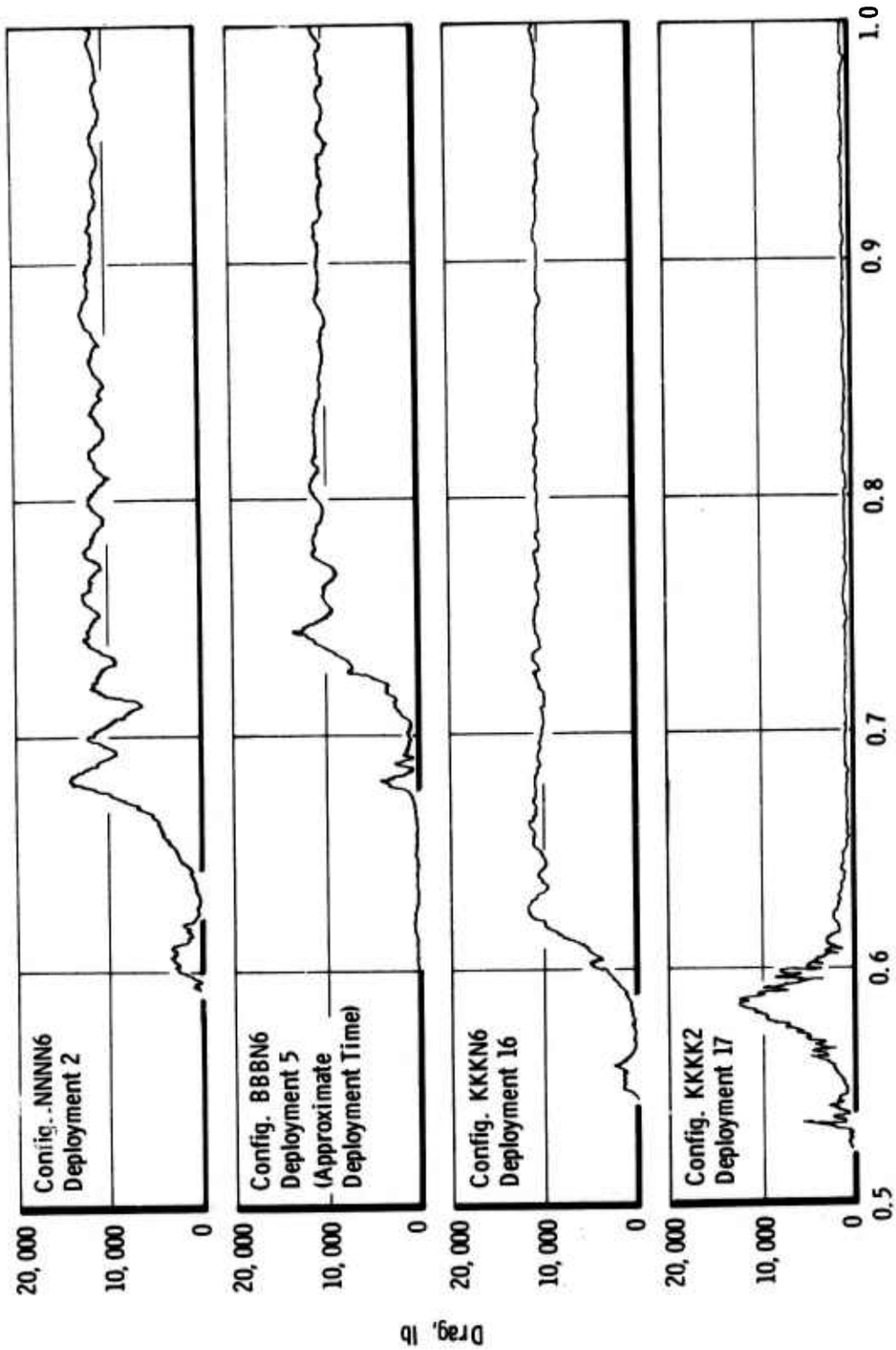

c. q_{∞_j} = 530 psf
Figure 9. Continued.

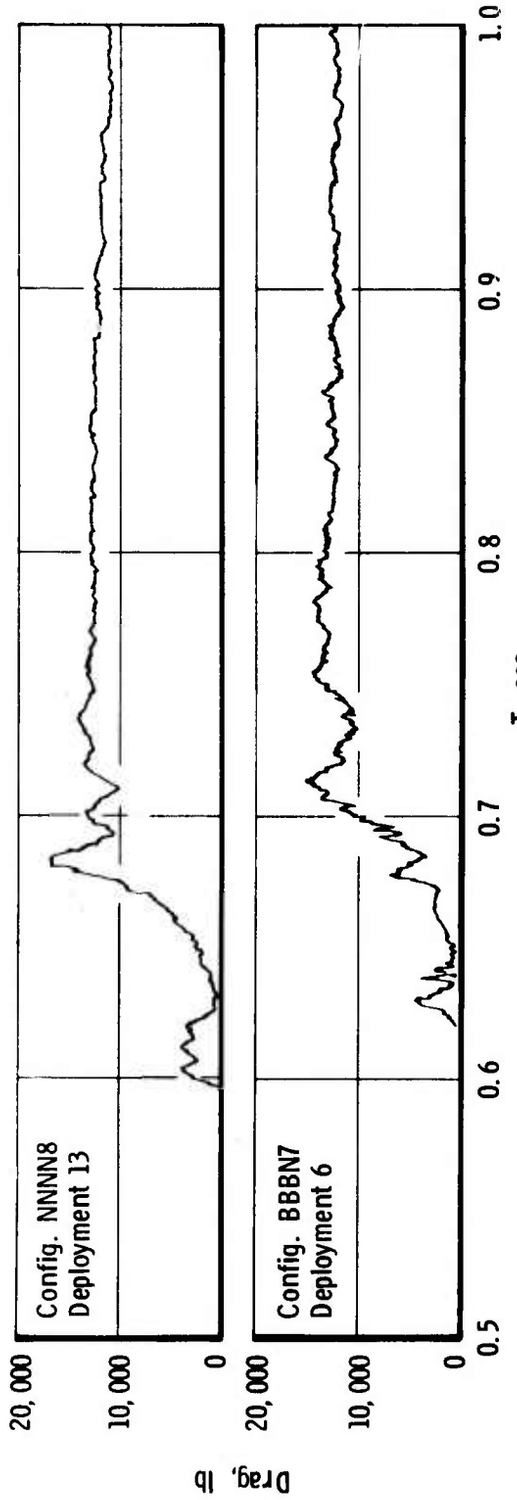

d. q_{∞_i} = 650 psf

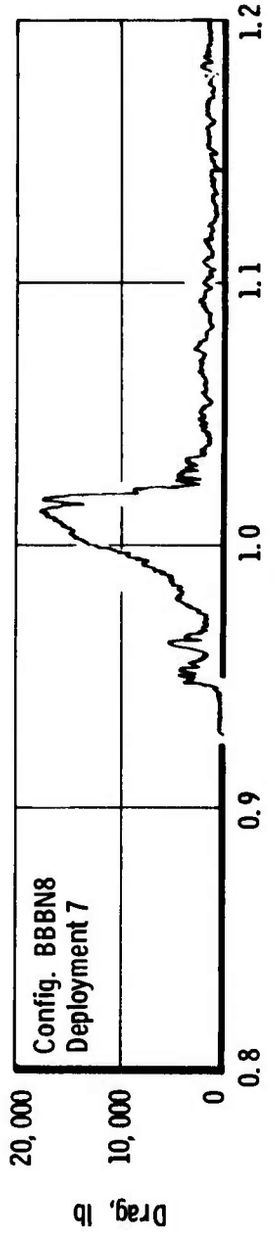

e. q_{∞_i} = 800 psf

Figure 9. Concluded.

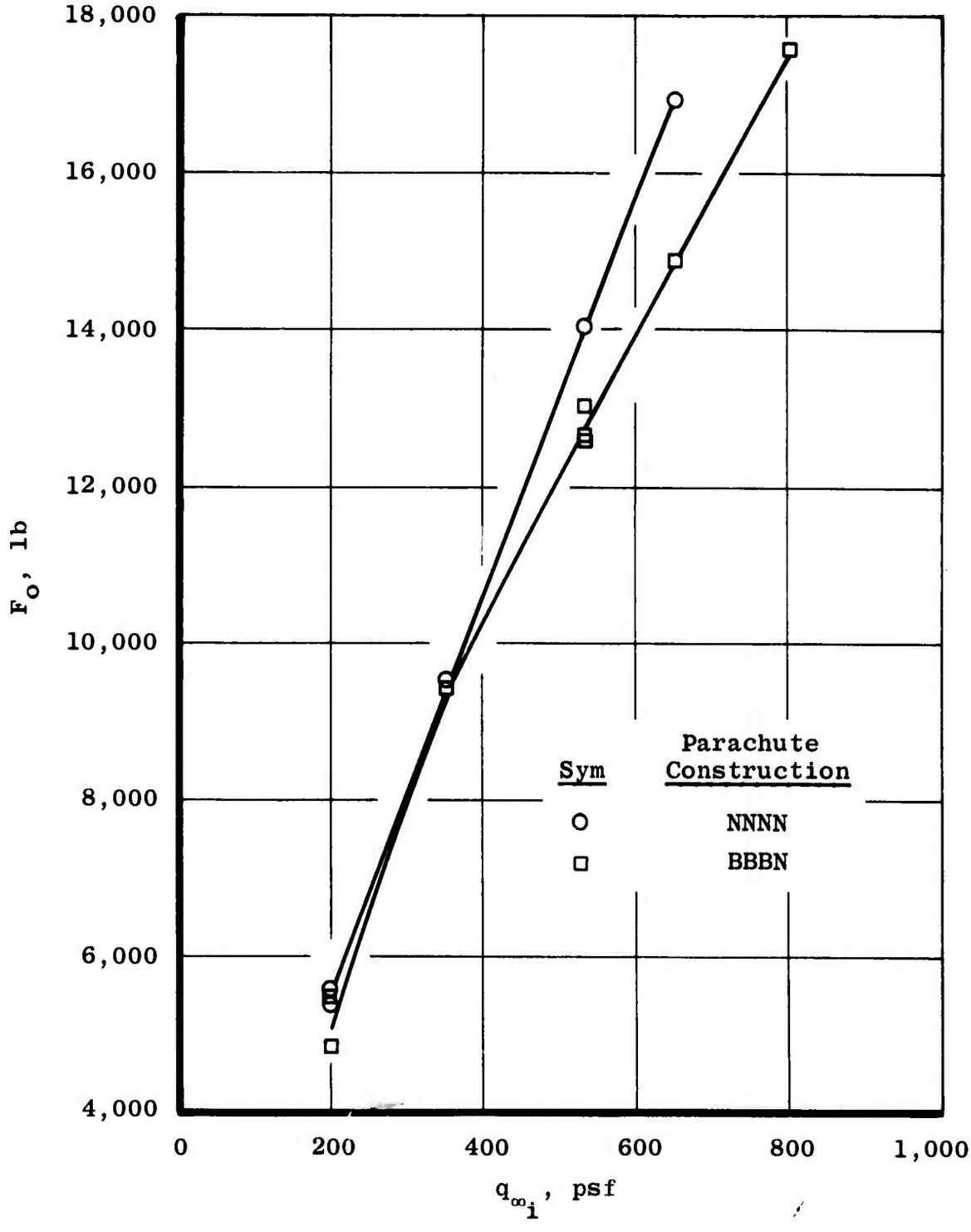

Figure 10. Variation of opening shock load with dynamic pressure, M_{∞_i} = 0.8.

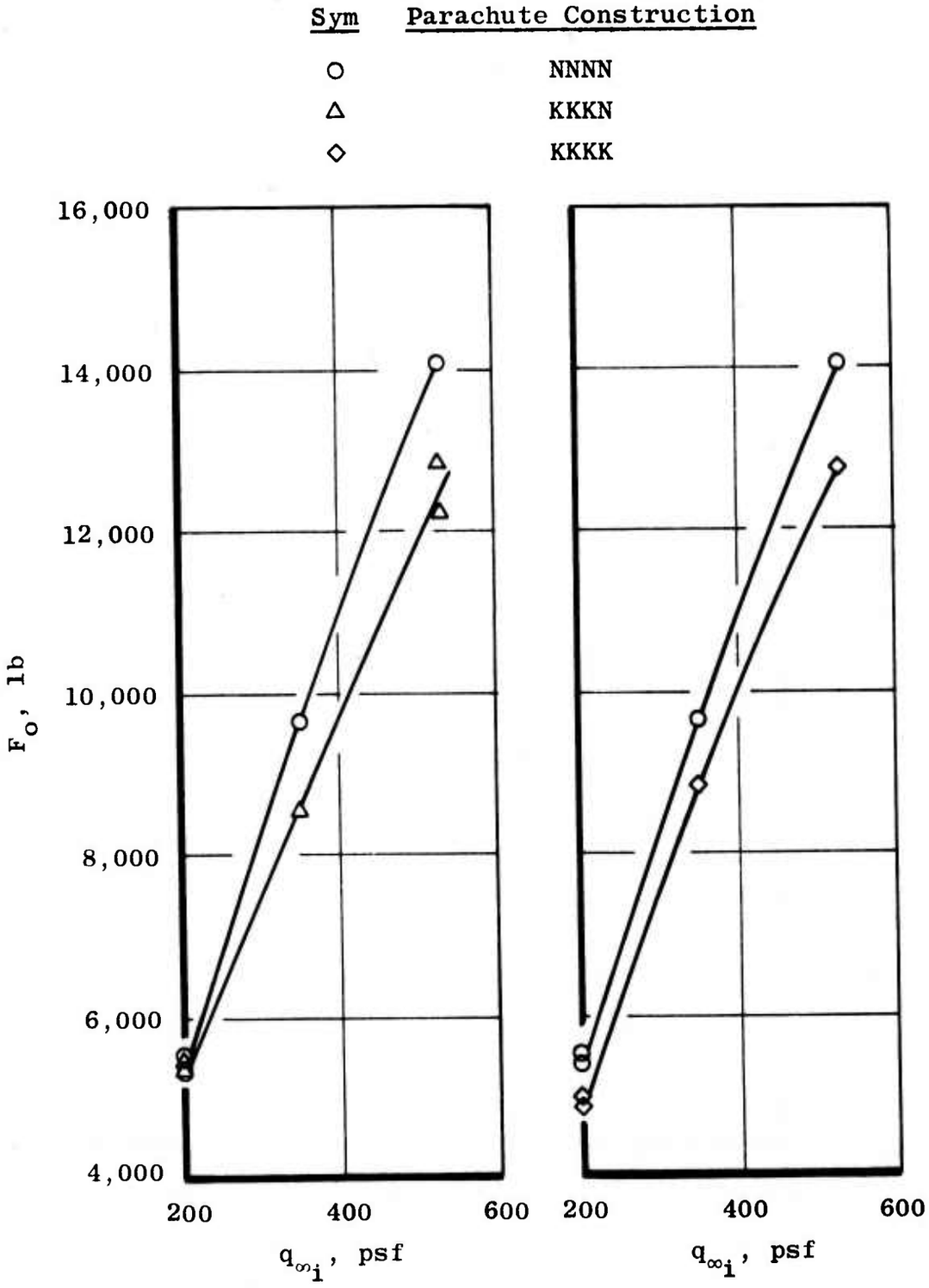

Figure 10. Concluded.

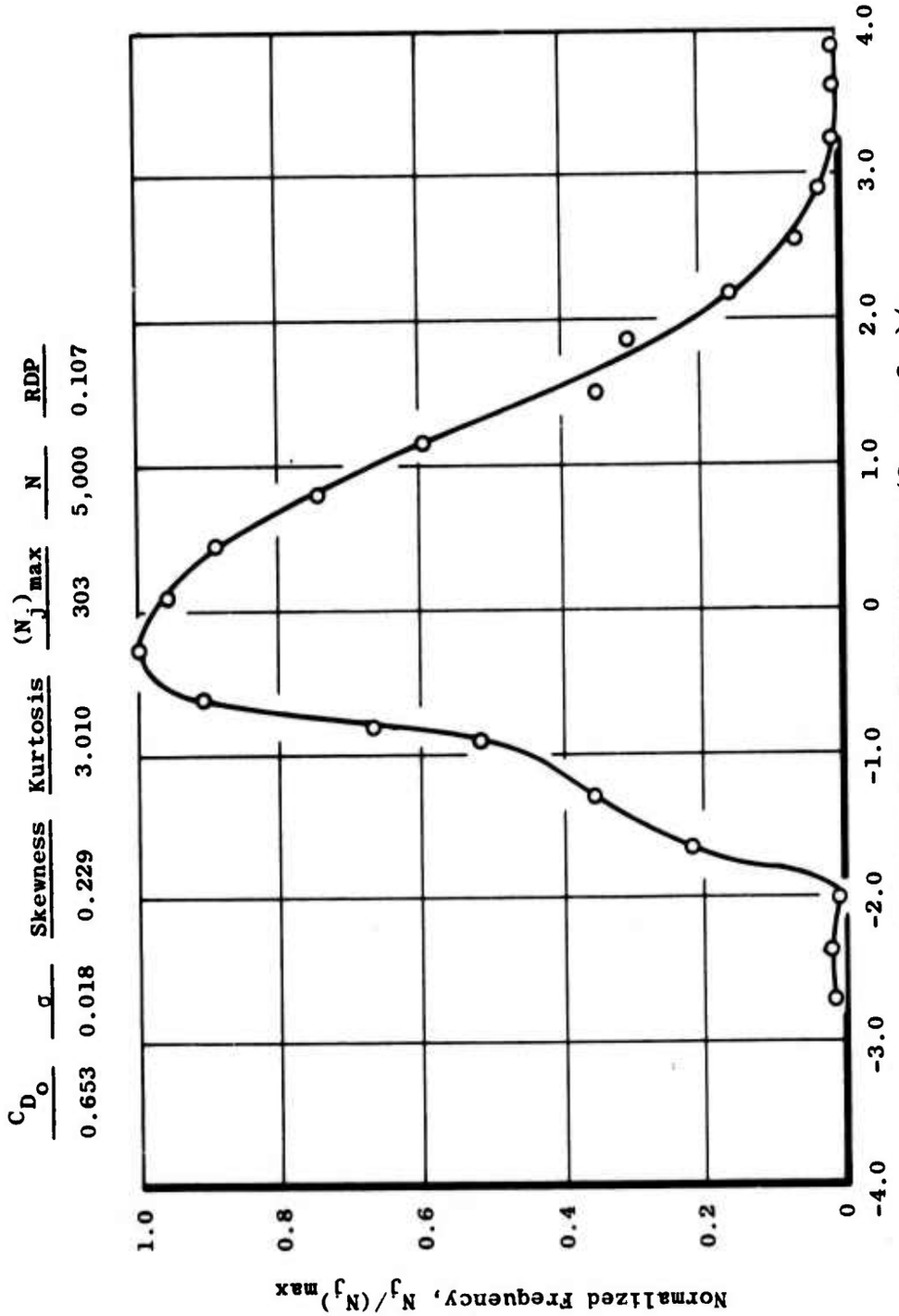

Figure 11. Typical distribution plot of the postinflation dynamic drag characteristics, $M_{\infty_j} = 0.8$, $q_{\infty_j} = 350$ psf, configuration BBBN5.

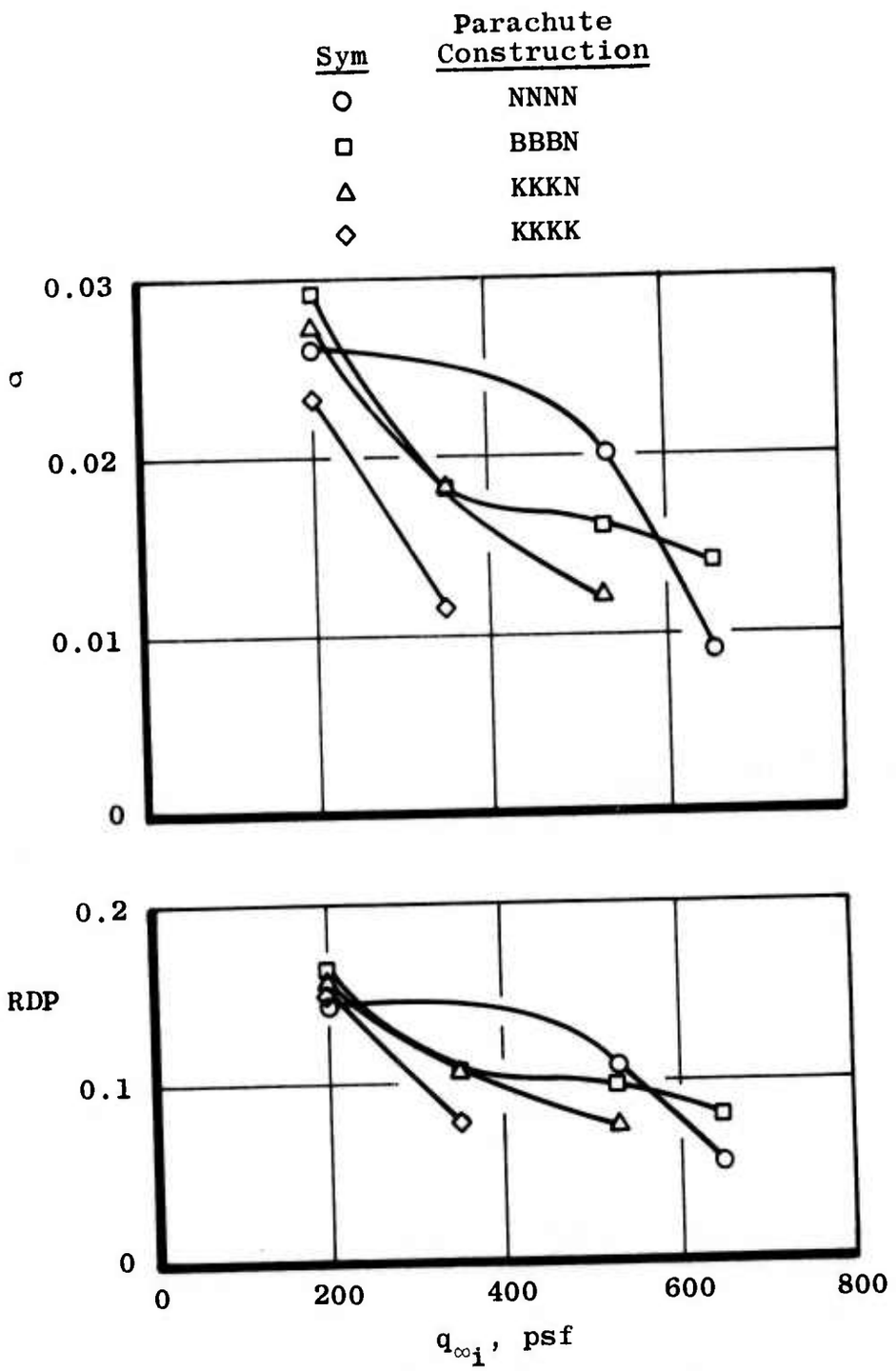

Figure 12. Relative dynamic parameter and standard deviation for the various parachute versions, M_{∞_i} = 0.8.

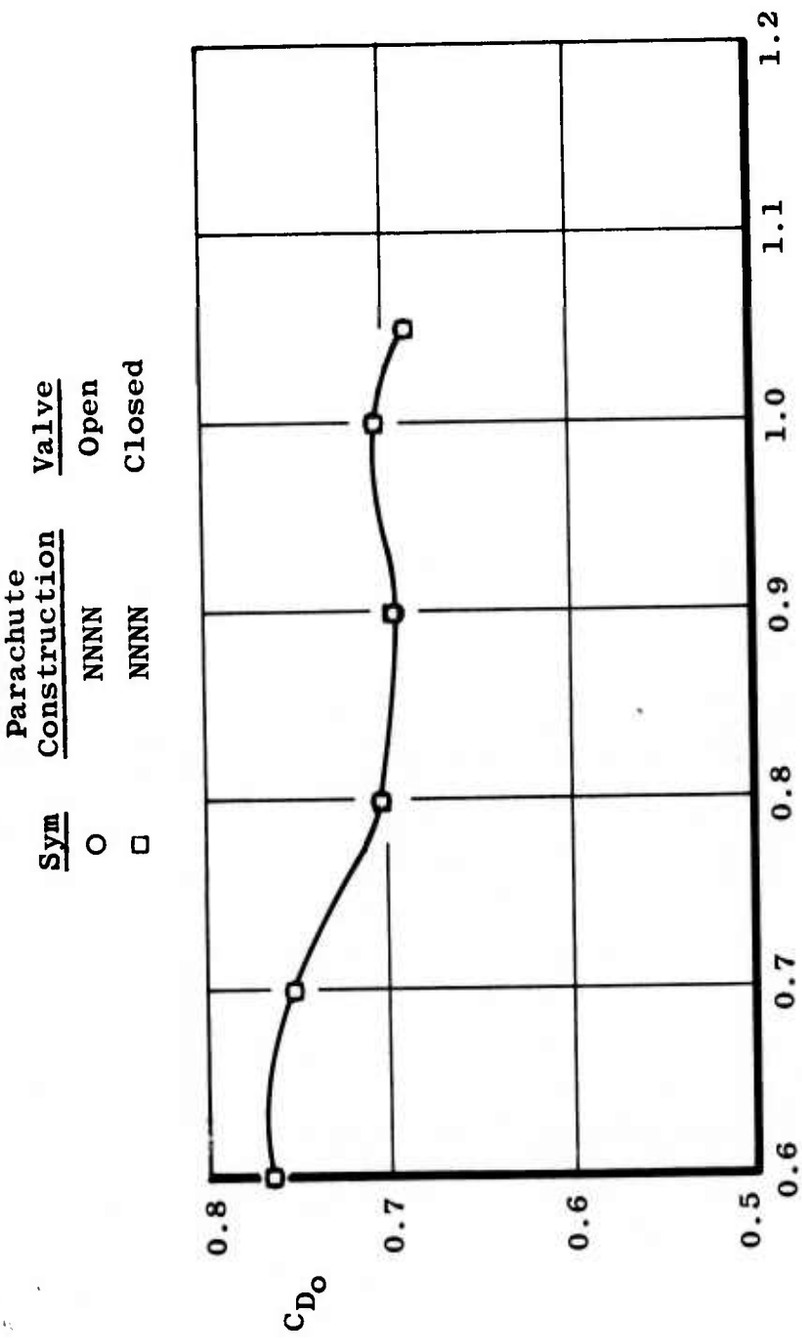

Figure 13. Effect of butterfly valve open and closed on parachute drag coefficient at various Mach numbers, q_∞ = 530 psf.

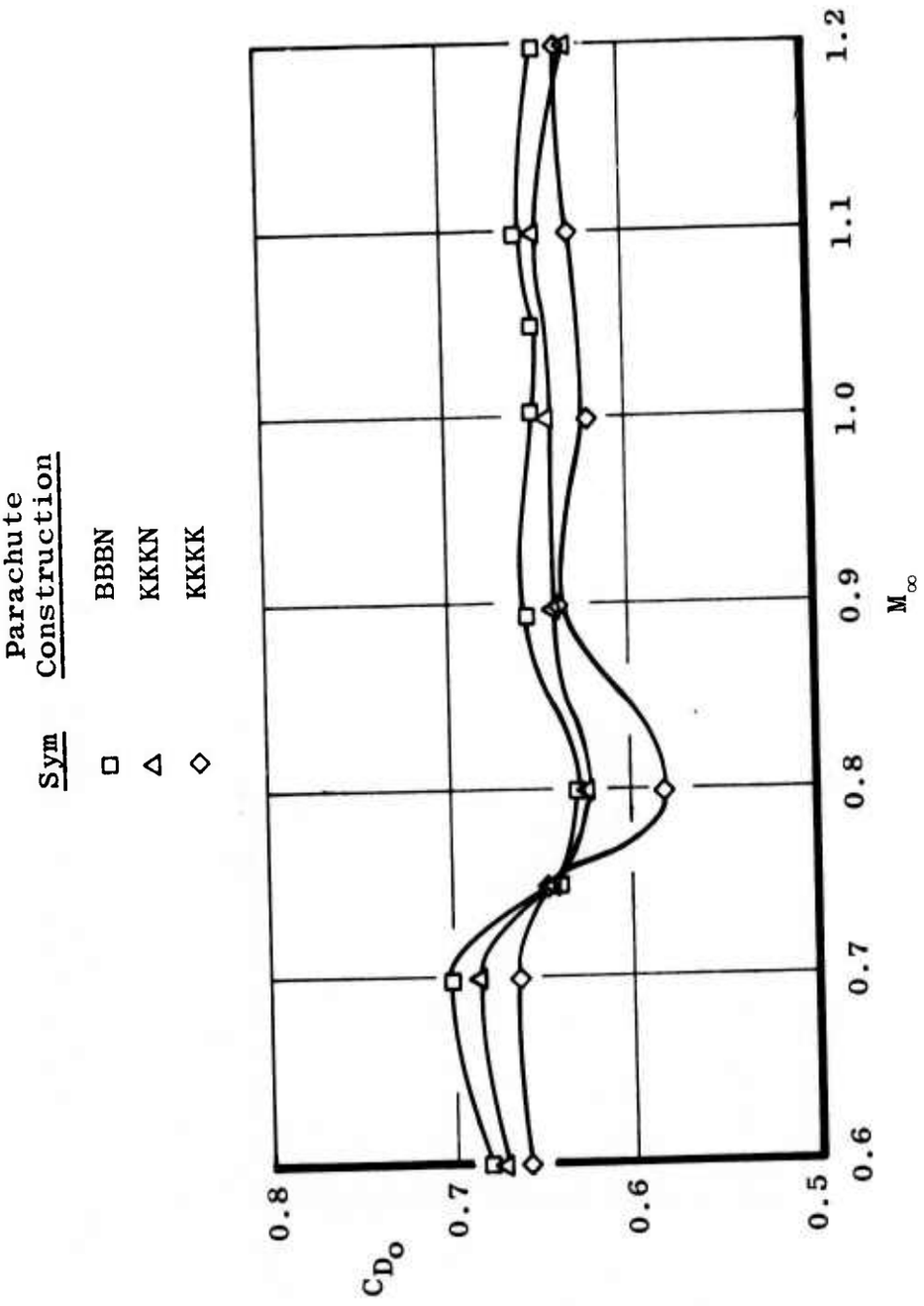

a. q_∞ = 200 psf

Figure 14. Variation of steady-state drag coefficient with Mach number.

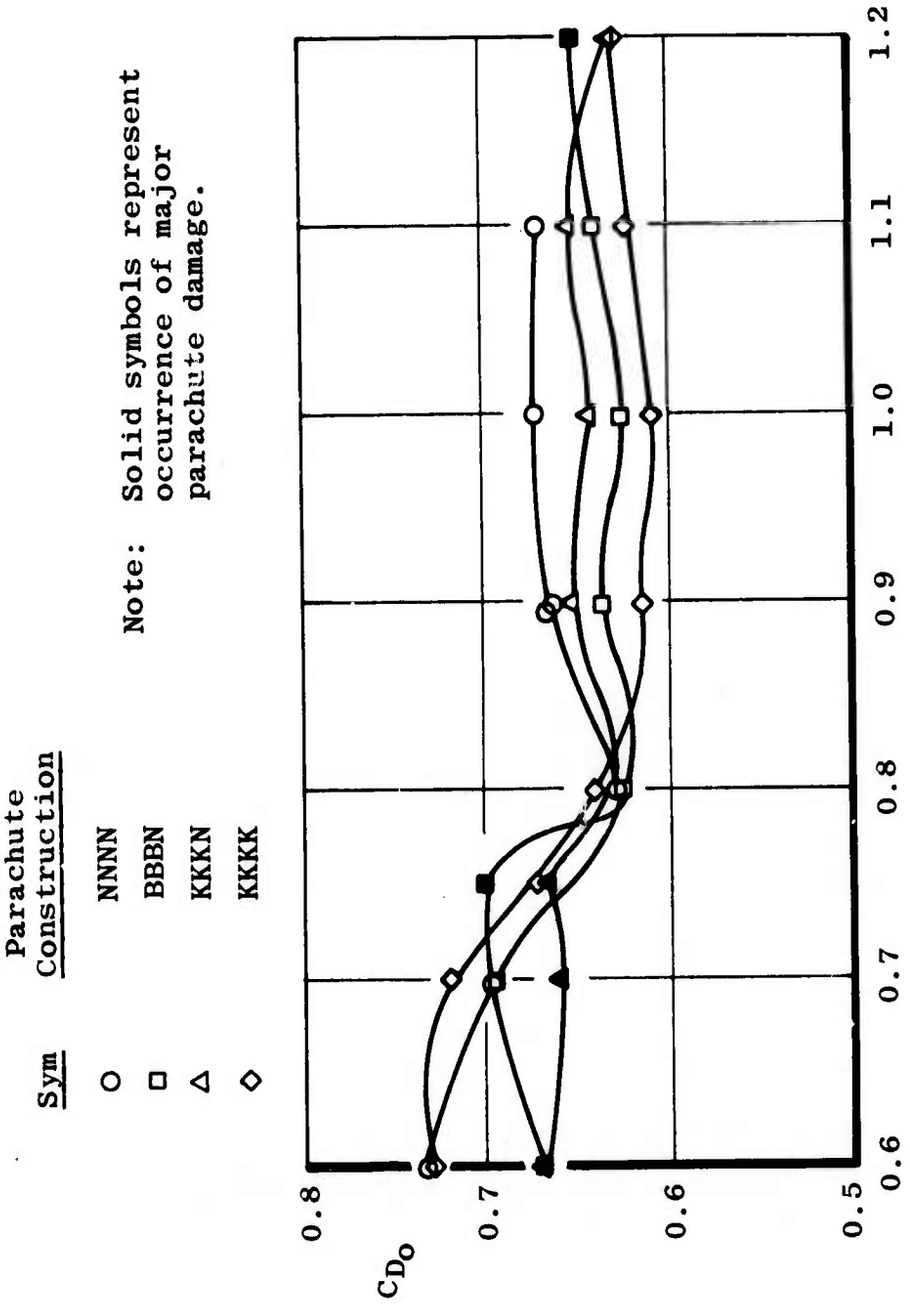

b. q_∞ = 350 psf
Figure 14. Continued.

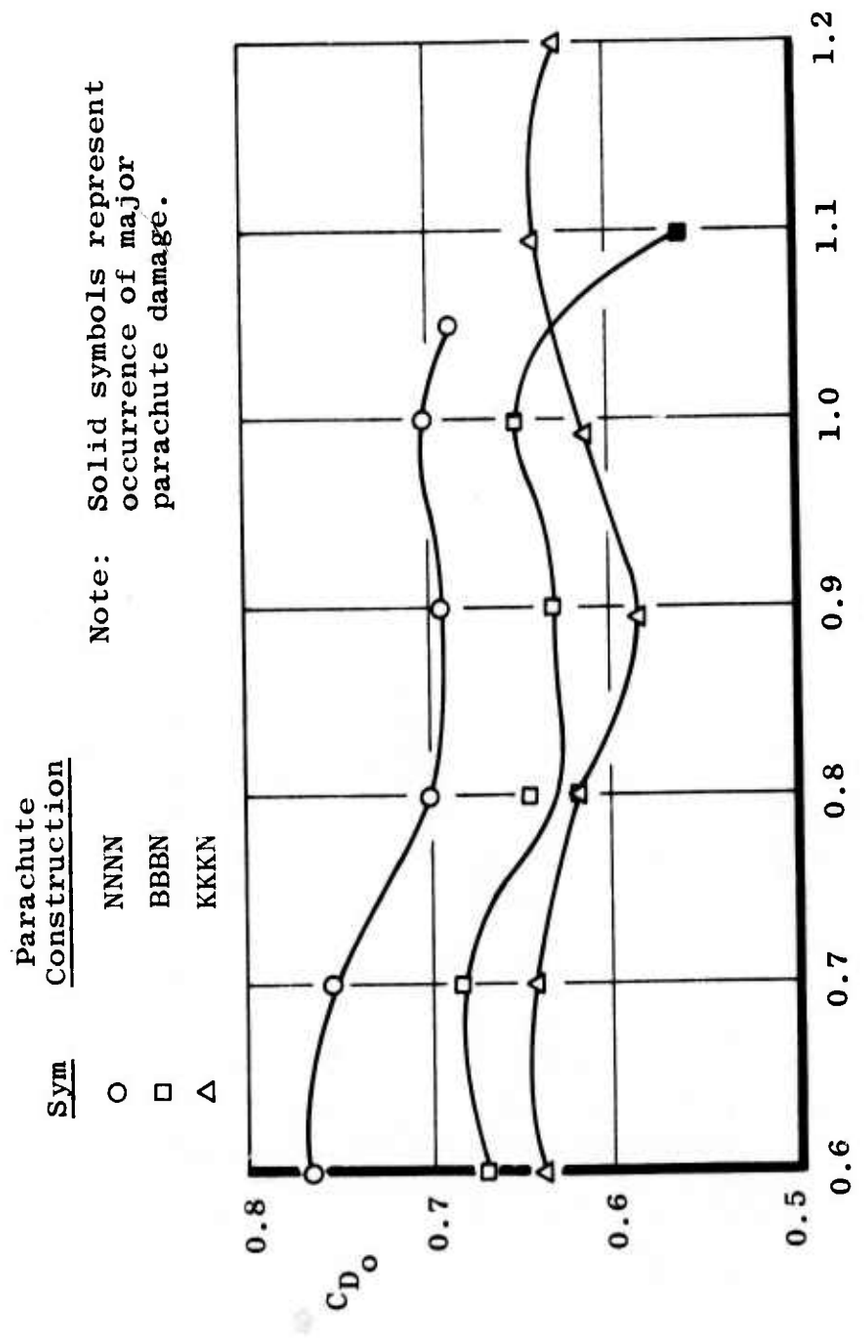

c. q_∞ = 530 psf
Figure 14. Continued.

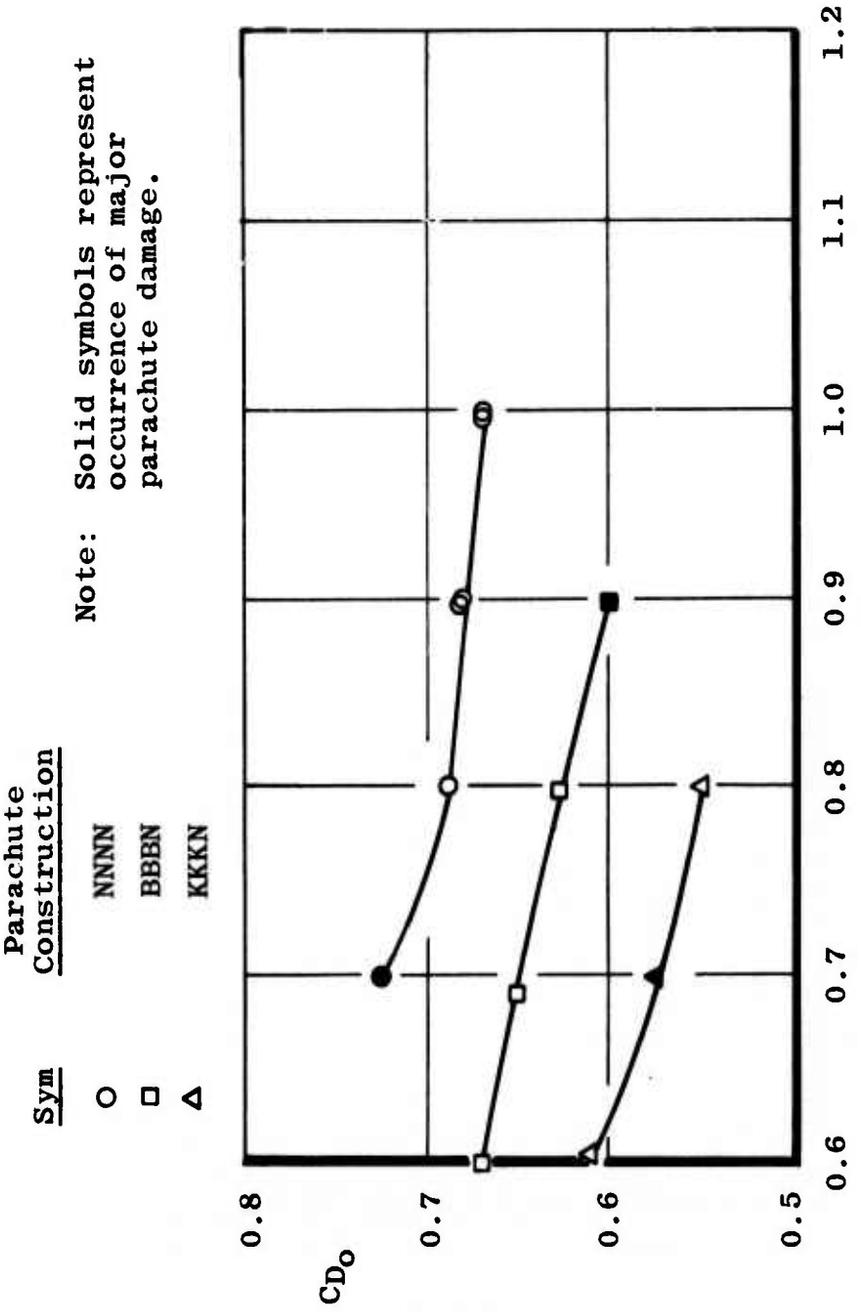

d. q_∞ = 650 psf
Figure 14. Concluded.

Sym	Parachute Construction
○	NNNN
◿	NNBN
◇	BNNN
◹	NBBN
□	BBBN
△	KKKN
◇	KKKK

Open Symbols: q_{∞_i} = 350 psf

Closed Symbols: q_{∞_i} = 530 psf

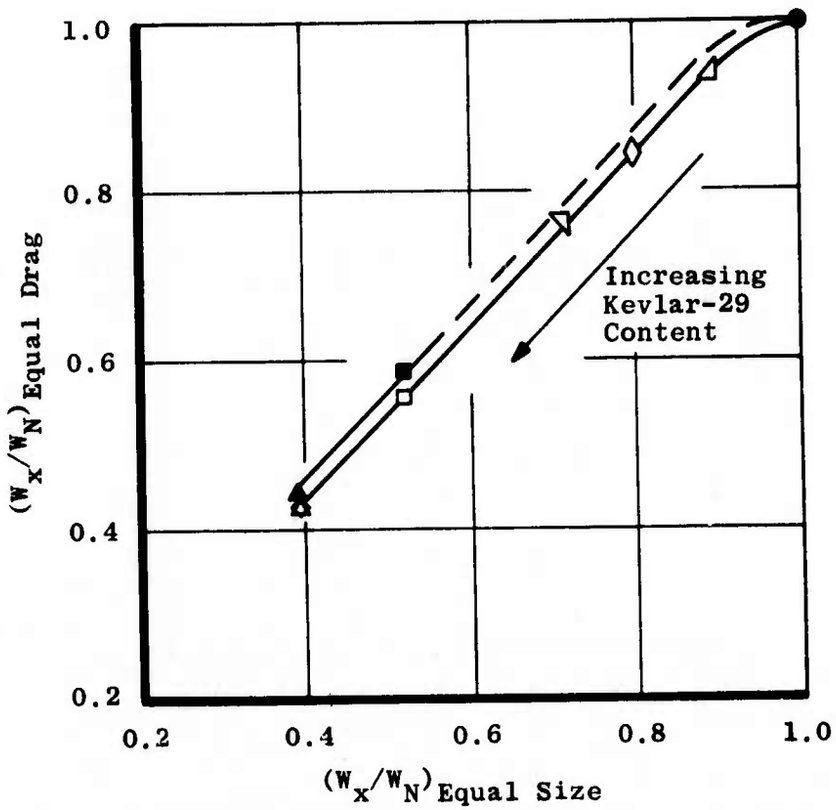

Figure 15. Weight comparison of equivalent drag-producing parachutes constructed of Kelvar-29 and/or nylon.

Sym	Parachute Construction
○	NNNN
◿	NNBN
◇	BNNN
◹	NBBN
□	BBBN
△	KKKN
◇	KKKK

Open Symbols: q_{∞_i} = 350 psf

Closed Symbols: q_{∞_i} = 530 psf

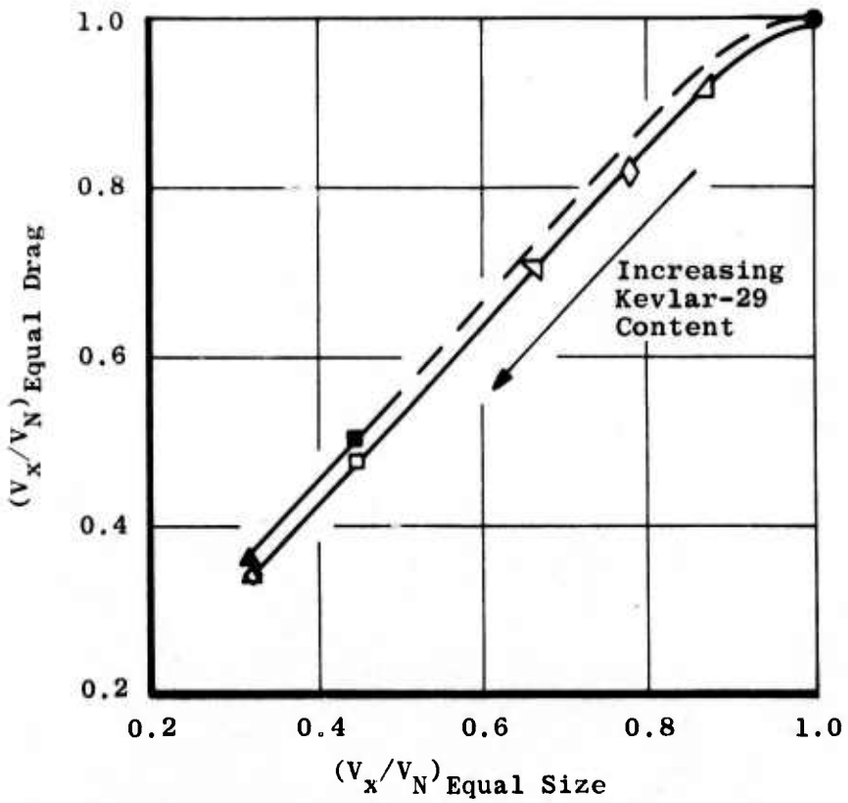

Figure 16. Volume comparison of equivalent drag-producing parachutes constructed of Kevlar-29 and/or nylon.

Table 1. Parachute Material Construction

CONFIGURATIONS	PARACHUTE CONSTRUCTION			
	NNNN5 NNNN6 NNNN7 NNNN8	BBBN5 BBBN6 BBBN7 BBBN8	KKKN5 KKKN6 KKKN7 KKKN8	KKKK1 KKKK2 KKKK3 KKKK4
MAJOR PARACHUTE COMPONENTS				
Radial Webs Horizontal Ribbons Suspension Lines Riser (Bridle) Webs	Nylon ↓	Kevlar-29 ↓ Nylon	Kevlar-29 ↓ Nylon	Kevlar-29 ↓
MINOR PARACHUTE COMPONENTS				
Vertical Tapes Vent Lines Vent Band Skirt Band Pocket Bands Keeper Sewing Thread/cord	Nylon ↓	Nylon ↓ Kevlar-29 Kevlar-29 Nylon Nylon	Kevlar-29 ↓ Nylon Kevlar-29	Kevlar-29 ↓

Table 2. Material Properties of Kevlar-29, Nylon, and Dacron Filaments

Item	Nylon	Dacron	Kevlar-29
Tensile Ultimate Strength, psi	117,000	106,000	400,000
Specific Gravity	1.14	1.38	1.44
Percent Elongation at Ultimate Strength	16 to 20	12 to 16	5 to 7
Zero-Strength Temperature, ^{o}F	473	473	850
50-Percent Ultimate Strength Temperature, ^{o}F	360	390	600

Note: Nylon and Dacron data obtained from E. I. Dupont Bulletin X-233 dated August 1971; Kevlar-29 data obtained from E. I. Dupont.

Table 3. Test Summary of Deployments

Configuration	Deployment Number	M_{∞_i}	q_{∞_i}, psf	F_o, lb
NNNN5	1	0.8	350	9,670
NNNN6	2	0.8	530	14,079
NNNN7*	3	0.8	650	13,085
BBBN5	4	0.8	350	9,416
BBBN6	5	0.8	530	13,069
BBBN7	6	0.8	650	14,900
BBBN8*	7	0.8	800	17,568
NNNN6	8	0.6	350	10,218
NNNN5	9	1.0	350	9,366
BBBN6	10	0.6	350	9,303
BBBN5	11	1.0	350	7,789
NNNN5	12	1.2	350	9,337
NNNNB	13	0.8	650	16,949
KKKN5	14	0.8	350	8,545
KKKK1	15	0.8	350	8,843
KKKN6	16	0.8	530	12,222
KKKK2*	17	0.8	530	12,781
KKKN7	18	0.8	200	5,479
KKKK3	19	0.8	200	5,056
BBBN6	20	0.8	200	4,856
NNNN6	21	0.8	200	5,517
BBBN5	22	0.8	200	5,451
KKKK4	23	0.8	200	4,872
KKKN8	24	0.8	200	5,401
KKKN7	25	0.8	530	12,831
NNNN6	26	0.8	200	5,396
BBBN6	27	0.8	530	12,567
BBBN7	28	0.8	530	12,644

*Major damage suffered at canopy inflation.

Table 4. Steady-State Performance Run Summary

Configuration	Deployment Number	Dynamic Pressure (q_∞), psf	Part Numbers by Mach Number								
			0.6	0.7	0.75	0.8	0.9	1.0	1.05	1.1	1.2
NNNN 5	12	350	54,64*	55,63*		56,62*	57,61*	58,60*		59	
NNNN 5	12	530	65,66*	67,68*		69,70*	71,72*	73,74*	75,76*		
NNNN 5	12	650		83		81,82*	79,80*	77,78*			
BBBN 5	22	200	132	133	139	130,140	134	135*	136*	137	138
BBBN 5	22	350	148	146	147	131,141	142	143		144	145
BBBN 6	27	530	219	218		216	217	224			
BBBN 7	28	530				229	230			231	
BBBN 6	27	650	220	221		222	223				
KKKN 8	24	200	178	179	180	176,181	182	183		184	185
KKKN 8	24	350	192	191	193	177,190	189	188		187	186
KKKN 7	25	530	199	200		198	201	202		203	204
KKKN 7	25	650	206		207	205					
KKKK 4	23	200	156	157	158	154	159	160		161	162
KKKK 4	23	350	170	169	168	155,167	166	165		164	163
KKKK 4	23	530	171								

*Butterfly Valve Closed

Table 5. Parachute Statistical Analysis Summary

Deployment Number	Average Drag Coefficient (C_{D_o})	Deviation (σ)	Skewness	Kurtosis	Total Number of Samples (N)	Relative Dynamic Parameter
1	----	----	----	----	----	----
2	0.712	0.020	0.340	3.078	5,000	0.107
3	----	----	----	----	----	----
4	0.653	0.018	0.229	3.010	5,000	0.107
5	0.635	0.016	-0.506	4.246	5,000	0.097
6	0.654	0.014	-0.162	2.757	5,000	0.080
7	----	----	----	----	----	----
8	0.742	0.025	0.391	2.594	5,000	0.126
9	0.762	0.033	0.072	2.580	5,000	0.164
10	0.674	0.012	-0.043	3.507	5,000	0.069
11	0.711	0.031	-0.022	2.399	5,000	0.164
12	0.773	0.017	0.048	2.702	4,999	0.087
13	0.613	0.009	0.505	3.300	4,998	0.055
14	0.639	0.018	-0.083	2.692	4,998	0.108
15	0.637	0.012	0.069	3.266	4,998	0.074
16	0.633	0.012	0.044	2.997	4,998	0.074
17	----	----	----	----	----	----
18	0.665	0.027	-0.145	2.558	4,998	0.152
19	0.700	0.058	0.826	2.584	5,000	0.275
20	0.667	0.028	-0.453	2.819	4,996	0.161
21	0.697	0.027	-0.387	2.351	4,996	0.132
22	0.668	0.026	-0.073	2.336	4,998	0.162
23	0.590	0.023	-0.437	3.442	4,998	0.149
24	0.601	0.024	-0.370	2.786	4,998	0.155
25	0.638	0.016	-0.358	2.816	4,998	0.098
26	0.636	0.026	-0.355	2.308	5,000	0.146
27	0.645	0.012	0.372	3.171	5,000	0.070
28	0.618	0.021	0.184	2.315	4,996	0.126

NOMENCLATURE

C_{D_o}	Parachute drag coefficient, $D/q_\infty S_o$
$C_{D_{oj}}$	Mean parachute drag coefficient value of each cell in the statistical analysis program, $D/q_\infty S_o$
D	Drag force, lb
F_o	Opening shock load, lb
M_∞	Tunnel free-stream Mach number
N	Total number of drag coefficient data samples used in the statistical analysis program
N_j	Number of drag coefficient data samples in each cell of the statistical analysis program
$(N_j)_{max}$	Maximum number of drag coefficient samples in any cell of the statistical analysis program
q_∞	Tunnel free-stream dynamic pressure, psf
RDP	Ratio of the 95-percent confidence level interval, expressed as drag coefficient interval, of a distribution of drag coefficient data to the average drag coefficient value as determined from the statistical analysis program
S_o	Nominal parachute reference area, 32.169 ft
V_N	Volume of nylon parachute configuration
V_x	Volume of any parachute configuration
W_N	Weight of nylon parachute configuration
W_x	Weight of any parachute configuration
X/D	Distance in forebody diameters (D = 17.6 in.) from model base to leading edge of parachute skirt, 9.024
σ	Standard deviation of the distribution of drag coefficient data determined from the statistical analysis program

SUBSCRIPTS

i	Conditions prior to parachute deployment
f	Conditions after parachute inflation